

*STRESS-DEFORMATION BEHAVIOR  
OF  
ANISOTROPIC BITUMINOUS MIXTURES*

*JANUARY, 1967*

*NO. 2*

*Joint  
Highway  
Research  
Project*

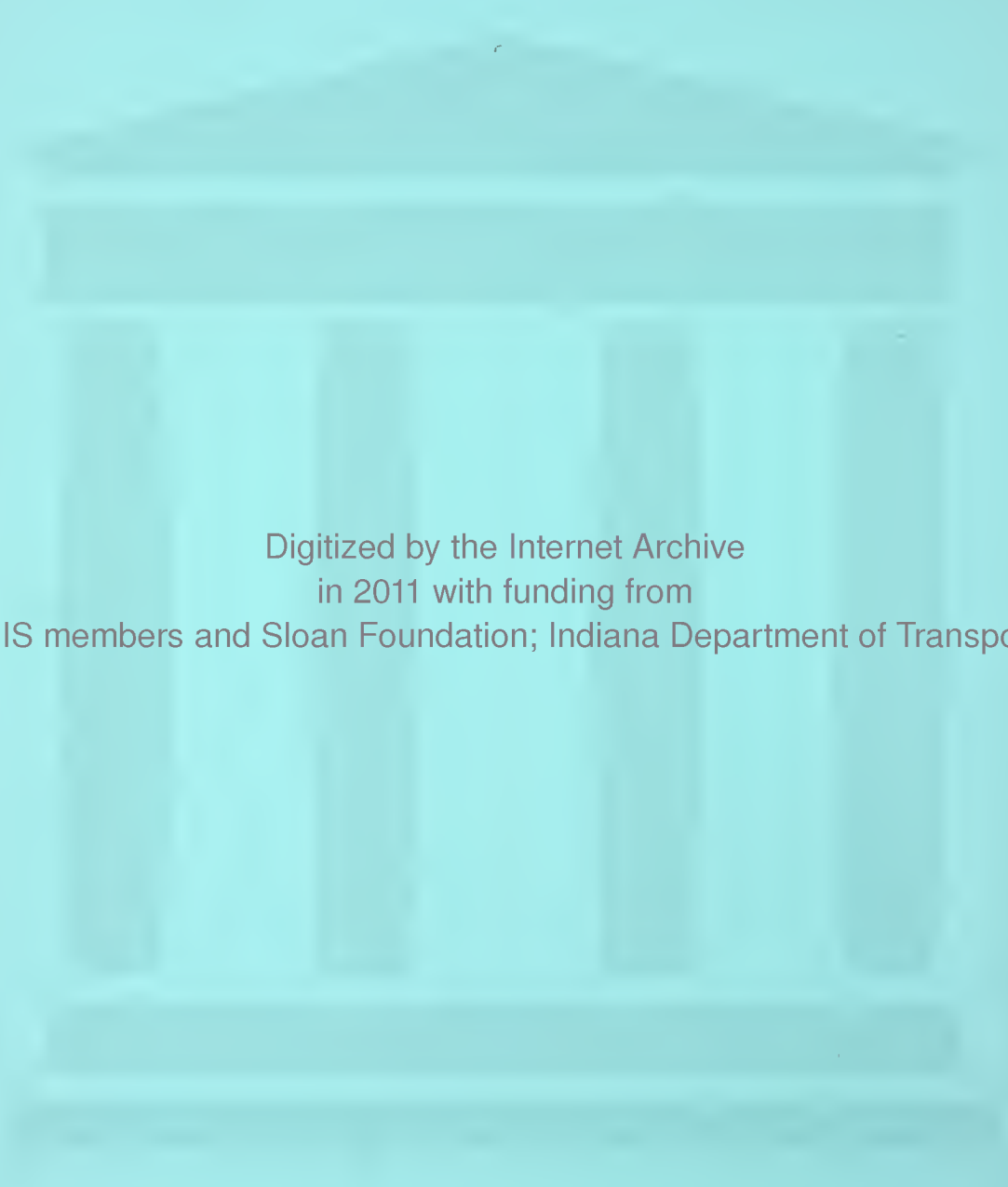
*by*

*H. W. BUSCHING*

*W. H. GOETZ*

*M. E. HARR*

*PURDUE UNIVERSITY  
LAFAYETTE INDIANA*



Digitized by the Internet Archive  
in 2011 with funding from  
LYRASIS members and Sloan Foundation; Indiana Department of Transportation

Technical Paper  
Stress-Deformation Behavior of Anisotropic  
Bituminous Mixtures

by

H. W. Busching, W. H. Goetz, M. E. Harr

Joint Highway Research Project

Project: C-36-8W

File: 2-5-23

Prepared as Part of an Investigation

Conducted by

Joint Highway Research Project  
Engineering Experiment Station  
Purdue University

in cooperation with

Indiana State Highway Commission

and the

Bureau of Public Roads  
U.S. Department of Commerce

Not Released for Publication

Subject to Change

Not Reviewed by

Indiana State Highway Commission

or the

Bureau of Public Roads

Purdue University  
Lafayette, Indiana  
January 1967

# STRESS-DEFORMATION BEHAVIOR OF ANISOTROPIC BITUMINOUS MIXTURES

by

H. W. Busching,\* W. H. Goetz,\*\* M. E. Harr\*\*\*

This is an advance copy of a paper to be presented at the Annual Meeting of the Association of Asphalt Paving Technologists to be held in Denver, Colorado, February 13, 14, 15, 1967. This advance copy is primarily to stimulate discussion. The paper is subject to modification and is not to be published as a whole or in part pending its release by the Association.

\* Assistant Professor of Civil Engineering, Clemson University,  
Clemson, South Carolina

\*\* Professor of Highway Engineering, Purdue University, Lafayette, Indiana

\*\*\* Professor of Soil Mechanics, Purdue University, Lafayette, Indiana

## SYNOPSIS

Bituminous mixture instability in the form of rutting and shoving, which sometimes occurs at signalized intersections, is indicative that present design methods, in some instances, need amplification with regard to predicting the stress-deformation response of mixtures. Also, the growing use of bituminous mixtures as structural layers in the pavement system makes it necessary to design them for specific applications other than as surface layers. The research reported here was an attempt to investigate concepts and laboratory tests that could be used to characterize the stress-deformation response of a particular bituminous mixture subjected to creep loads of various magnitudes applied over a range of temperatures. New concepts of design were advanced which would permit prediction of the deformation of the mixture under conditions that include, among other possible factors, various magnitudes of load and a range of test temperatures as well as possible anisotropy of the mixture.

A hypothesis concerning the mechanistic description of a deformable, transversely anisotropic bituminous mixture was formulated and tested under controlled conditions in the laboratory. Results indicated that invariant material coefficients exist, for the conditions of laboratory testing chosen, which would assist prediction of the magnitude of deformations which result when imposed stress conditions are known. Parameters measured included stiffnesses, shear moduli and Poisson's ratios for various orientations within a compacted bituminous mixture. Test results for the mixture compacted in the laboratory confirmed the anisotropic nature of the mixture. The methods of this investigation provided

quantitative parameters that relate the common engineering concepts of stress and strain. These parameters can be used in the description, evaluation and design of bituminous mixtures for the prefailure conditions considered in the testing program.

The concepts and parameters verified in laboratory testing have possible use in proportioning constituents of bituminous mixtures as well as in unifying mixture design and pavement design concepts.



## STRESS-DEFORMATION BEHAVIOR OF ANISOTROPIC BITUMINOUS MIXTURES

by  
H. W. Busching,\* W. H. Goetz\*\* and M. E. Harr\*\*\*

### INTRODUCTION

Bituminous mixtures are being used in highways as load-distributing layers, as well as wearing courses. In these applications both the asphalt and the aggregate serve as structural elements. Recently emphasis has been placed upon specifying more exactly the role of bituminous materials and mixtures when used in any position in a layered system.

In some instances, pavement distress at signalized intersections takes the form of rutting and shoving of the bituminous mixture. Sometimes this occurs even when mixture design methods have indicated the mixture to be stable. Figure 1 shows an example of this type of distress.

In general, methods currently used to design bituminous mixtures in the laboratory are not completely suitable for predicting the response of the pavement to load in useful engineering units such as stress and strain. In addition to this, mixture design methods do not distinguish between mixtures that will be used as flexible pavement layers and mixtures that will be used as overlays on rigid pavements (17). It is the purpose of this paper to introduce new concepts in mixture evaluation and to show their relevance to the unification of mixture design and pavement design.

\* Assistant Professor of Civil Engineering, Clemson University, Clemson, South Carolina

\*\* Professor of Highway Engineering, Purdue University, Lafayette, Indiana

\*\*\* Professor of Soil Mechanics, Purdue University, Lafayette, Indiana



FIGURE 1. RUTTING AND SHOVING OF A BITUMINOUS MIXTURE AT A SIGNALIZED INTERSECTION.



At present, no single theory of material behavior which considers time-and temperature-dependent characteristics of bituminous mixtures is widely used in the design of flexible pavements. It is recognized, however, that bituminous mixtures are both time-and temperature-dependent (12, 18, 19, 28). Evaluation of the dependence of bituminous mixture deformation on time and temperature is important in predicting mixture behavior under traffic-load-associated as well as non-traffic-load-associated stresses.

Because bituminous mixtures are placed in layers that differ on the basis of composition, thickness and state of compaction, it is reasonable to expect that the mixture will behave as an anisotropic material. Hence, deformation response of the mixture to stress will be direction-dependent. Researchers in bituminous mixture behavior, (3, 14, 21), soil mechanics, (1, 22), and other disciplines (4,5,6,7,8,9,13,25,27) have noted that the stiffness of materials is often different in the vertical direction than it is in the horizontal direction. Figure 2 shows the stress distribution pattern under a concentrated load acting on a semi-infinite, elastic, transversely anisotropic material (16). It is apparent that the structural adequacy of a bituminous mixture must be assessed with recognition of possible anisotropy.

The research presented here is one part of an investigation to evaluate in quantitative units, common to both mixture and pavement design, the stress-deformation response of a bituminous mixture under controlled conditions in the laboratory. The investigation utilizes basic principles of mechanics of deformable bodies to describe the response of the mixture. Analysis and laboratory tests were complementary and were performed to describe and characterize the stress-deformation response of the mixture with full recognition of its possible anisotropy as well as its time and temperature-dependent deformation.

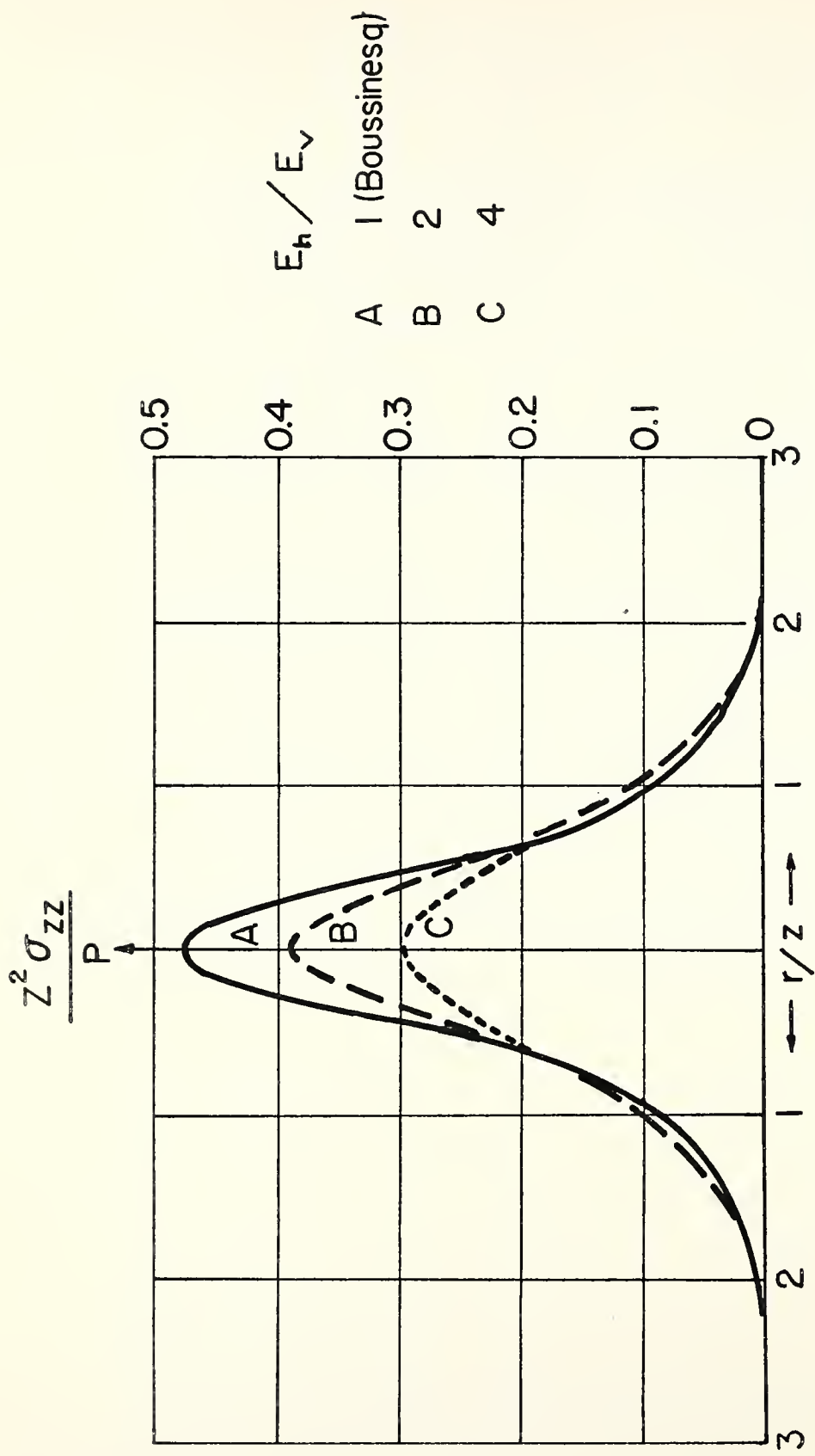


FIGURE 2 VERTICAL STRESS DISTRIBUTION PATTERN  $(\sigma_{zz})$  UNDER A CONCENTRATED LOAD  $(P)$  ACTING ON A SEMI-INFINITE, ELASTIC, TRANSVERSELY ANISOTROPIC MATERIAL (AFTER LGM MEDEDELINGEN).  $E_h$  IS HORIZONTAL COMPONENT OF YOUNG'S MODULUS,  $E_v$  IS VERTICAL COMPONENT.

## DEVELOPMENT OF THEORY

The investigation reported here is deterministic and phenomenological. It was generated on a theoretical basis by the assumption that stress-deformation relationships for a bituminous mixture would be amenable to deterministic analysis. Hence, it was desired to measure output strains, as shown in Figure 3, when input stresses were known. The transfer functions which would permit the deformation response of the mixture to be predicted were to be determined.

The practical soundness for this type of investigation is exemplified by elasticity and viscoelasticity theories for linearly elastic and viscoelastic materials (20,23,24,26). Further support for the analysis may be noted from the example which follows.

Assume that the total deformation of a bituminous mixture is a function of time and temperature as well as other independent variables that may include mixture constituents. The incremental change in deformation may then be expressed as a total differential as follows:

$$du(t, T, \sigma, AC, \dots) = \frac{\partial u}{\partial t} dt + \frac{\partial u}{\partial T} dT + \frac{\partial u}{\partial \sigma} d\sigma + \frac{\partial u}{\partial (AC)} d(AC) + \dots \quad (1)$$

where  $t$  = time

$\sigma$  = stress

AC = asphalt content

The number of independent variables may be very large and may include such factors as stearic hardening, amount of filler or type of filler,

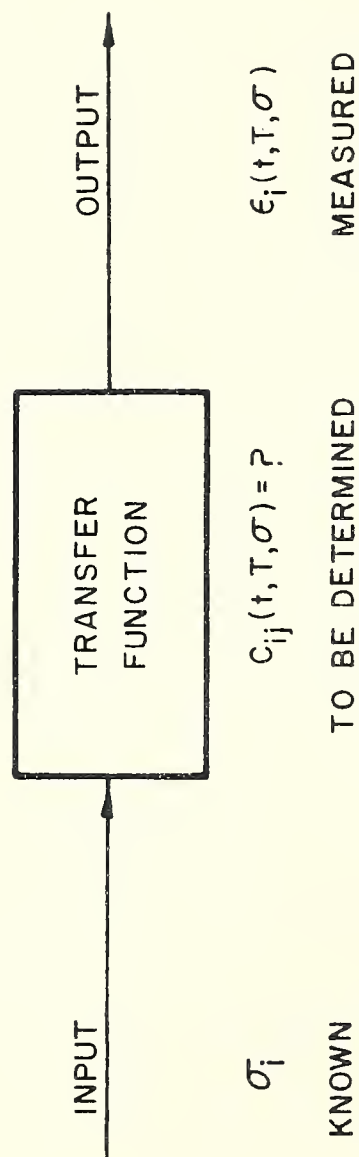


FIGURE 3. SCHEMATIC DIAGRAM OF DETERMINISTIC PROCESS

provided these factors contribute some measureable output. It is possible that the effects of some of the variables are amenable to superposition theories analogous to the superposition of time and temperature in the theory of linear viscoelasticity (2).

In this study, deformation was related specifically to stress magnitude, time and temperature. While it was recognized that truncation of the series shown in Equation 1 would introduce some error into the validity of applying the relations obtained in the laboratory to field problems, the discrepancies did not appear to be as restrictive as those of currently-used design methods. Further studies will be needed to evaluate the significance of truncation. As far as possible, other factors that might have influenced deformation were kept constant.

It was assumed that the compacted bituminous mixture tested in the laboratory was statistically homogeneous and transversely anisotropic.

A transversely anisotropic material has one axis of rotational symmetry. Hence a rotation transformation about one axis of the material element, as shown in Figure 4, establishes congruence between the edges and faces of the element in its initial and final positions. The assumptions of homogeneity and anisotropy are compatible with observations of bituminous mixtures tested in the laboratory (14,21).

Also implicit in the testing is the assumption that the typical element considered in the course of testing is representative of the larger prototype composed of many similar typical elements. The elements that were considered in the course of testing had finite dimensions although it was assumed that infinitesimal differential theories of material behavior would hold for this element as well as for a body composed of many identical elements.



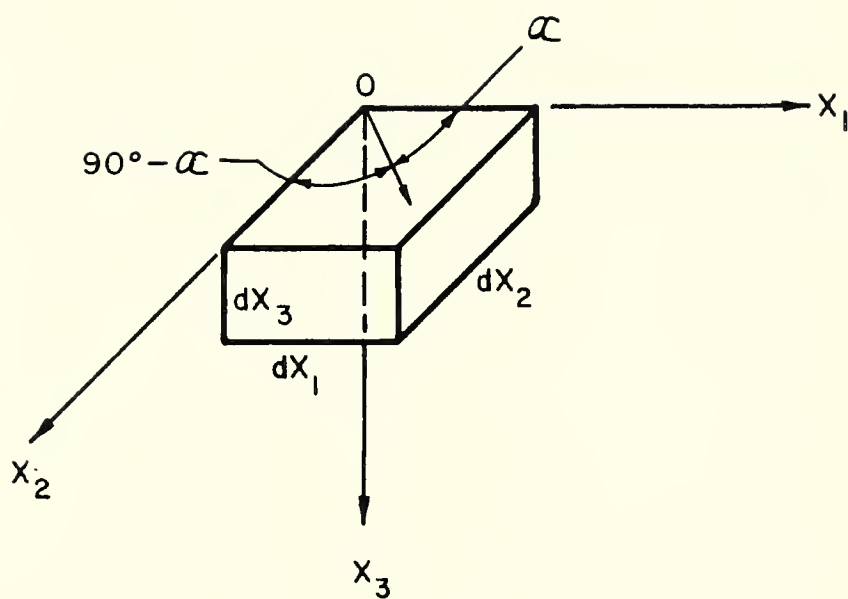


FIGURE 4. TYPICAL ELEMENT AND COORDINATE SYSTEM

To simplify notation, the following equivalence relations are used throughout the report:

$$\begin{bmatrix} \sigma_1 & \sigma_6 & \sigma_5 \\ \sigma_6 & \sigma_2 & \sigma_4 \\ \sigma_5 & \sigma_4 & \sigma_3 \end{bmatrix} = \begin{bmatrix} \sigma_{11} & \sigma_{12} & \sigma_{13} \\ \sigma_{21} & \sigma_{22} & \sigma_{23} \\ \sigma_{31} & \sigma_{32} & \sigma_{33} \end{bmatrix} = S$$

$$\begin{bmatrix} \epsilon_1 & \epsilon_6 & \epsilon_5 \\ \epsilon_6 & \epsilon_2 & \epsilon_4 \\ \epsilon_5 & \epsilon_4 & \epsilon_3 \end{bmatrix} = \begin{bmatrix} \epsilon_{11} & \frac{\epsilon_{12}}{2} & \frac{\epsilon_{13}}{2} \\ \frac{\epsilon_{21}}{2} & \epsilon_{22} & \frac{\epsilon_{23}}{2} \\ \frac{\epsilon_{31}}{2} & \frac{\epsilon_{32}}{2} & \epsilon_{33} \end{bmatrix} = E$$

Graphical definition of the stresses,  $\sigma_{ij}$ , and strains,  $\epsilon_{ij}$ , as well as the location of the coordinate axis with respect to the compacted bituminous mixture are given in the Appendix.

Since deformations,  $u_i$ , are related to strains,  $\epsilon_{ij}$ , by the relationship  $\epsilon_{ij} = \frac{\partial u_i}{\partial x_j}$ , it was found convenient to hypothesize that the probable form of the stress-deformation relationship would be equivalent to a stress-strain relationship. When stress is considered to be a function of six independent strains, then it is possible to expand any stress component in a Taylor's series of a function of the six strains. Hence, we find, for example,  $\sigma_1$ , as follows:

$$\sigma_1(\epsilon_1, \epsilon_2, \epsilon_3, \epsilon_4, \epsilon_5, \epsilon_6) = \sigma_1(\epsilon_1, \epsilon_2, \epsilon_3, \epsilon_4, \epsilon_5, \epsilon_6) \Big|_0 +$$

$$\frac{\partial \sigma_1}{\partial \epsilon_1} (\epsilon_1 - 0) + \frac{\partial \sigma_1}{\partial \epsilon_2} (\epsilon_2 - 0) + \frac{\partial \sigma_1}{\partial \epsilon_3} (\epsilon_3 - 0) + \frac{\partial \sigma_1}{\partial \epsilon_4} (\epsilon_4 - 0) + \frac{\partial \sigma_1}{\partial \epsilon_5} (\epsilon_5 - 0) + \frac{\partial \sigma_1}{\partial \epsilon_6} (\epsilon_6 - 0) + \dots$$

For purposes of the experiment it was found convenient to neglect the term  $\sigma_1(\epsilon_1 \dots \epsilon_6) \Big|_0$ . Since this term is comparable to the prestress that exists in the material, it was not evaluated and generally is not considered in pavement construction except indirectly through type and amount of compaction, gradation and other factors. Because compaction procedures were uniform throughout the study, the prestress term was the same for all cases.

If only small strains are considered, then products of strains are much smaller than linear combinations of the strains and therefore may be neglected. These assumptions reduce the stress-strain relationships to those commonly referred to as Cauchy's generalization of Hooke's law. Its form is

$$S = C'E \quad (2)$$

where  $S$  is the column vector  $(\sigma_1, \sigma_2, \sigma_3, \sigma_4, \sigma_5, \sigma_6)$ ,  $E$  is the column vector  $(\epsilon_1, \epsilon_2, \epsilon_3, \epsilon_4, \epsilon_5, \epsilon_6)$  and  $C'$  is the matrix of elements that relate stress to strain.

$$C' = \begin{bmatrix} c_{11} & c_{12} & c_{13} & c_{14} & c_{15} & c_{16} \\ c_{21} & c_{22} & c_{23} & c_{24} & c_{25} & c_{26} \\ c_{31} & c_{32} & c_{33} & c_{34} & c_{35} & c_{36} \\ c_{41} & c_{42} & c_{43} & c_{44} & c_{45} & c_{46} \\ c_{51} & c_{52} & c_{53} & c_{54} & c_{55} & c_{56} \\ c_{61} & c_{62} & c_{63} & c_{64} & c_{65} & c_{66} \end{bmatrix}$$

The relationship in Equation 2 may be rewritten as follows:

$$E = CS \quad (3)$$

where  $C$  is the inverse of matrix  $C'$ . This particular form of the matrix equation was used in this investigation.

The elements of matrix C are coefficients that relate stress to strain and are functions of time and temperature as well as other variables. In general, there are 36 coefficients to evaluate for the most anisotropic material. Since the problem was simplified by the assumption of transverse anisotropy, the number of material coefficients can be further reduced. The reduction is accomplished by use of the following rotation transformations:

$$\begin{aligned} S' &= ASA^T \\ E' &= AEA^T \end{aligned} \quad (4)$$

where A is the matrix of direction cosines formed as follows:

		Old Coordinate System		
New Coordinate System		$X_1$	$X_2$	$X_3$
	$X'_1$	$a_{11}$	$a_{12}$	$a_{13}$
	$X'_2$	$a_{21}$	$a_{22}$	$a_{23}$
	$X'_3$	$a_{31}$	$a_{32}$	$a_{33}$

$a_{ij} = \cos(X'_i, X_j)$

$A^T$  is the transpose of the direction cosine matrix.

The relations for the transformed strains

$$\begin{aligned} \epsilon'_{ij} &= \epsilon'_{ij} \left[ \sigma'_{ij} (\sigma_{ij}) \right] \\ \epsilon'_{ij} &= \epsilon'_{ij} \left[ \epsilon_{ij} (\sigma_{ij}) \right] \end{aligned} \quad (5)$$

were computed by using the equations of rotation transformation and the generalized expression of stress-strain response given by Equation 3. From these relations (Equation 5) it is possible to make identifications between invariant functions involving strains in the original and rotated coordinate systems. The matrix of material coefficients for a transversely anisotropic material is given as follows:

$$C = \begin{bmatrix} c_{11} & c_{12} & c_{13} & 0 & 0 & 0 \\ c_{12} & c_{11} & c_{13} & 0 & 0 & 0 \\ c_{31} & c_{31} & c_{33} & 0 & 0 & 0 \\ 0 & 0 & 0 & c_{44} & 0 & 0 \\ 0 & 0 & 0 & 0 & c_{44} & 0 \\ 0 & 0 & 0 & 0 & 0 & 2(c_{11}-c_{12}) \end{bmatrix} \quad (6)$$

This matrix of coefficients differs from that given previously by Love (15) and Hearmon (8) for transversely anisotropic elastic materials. Because the matrix is not symmetric it contains six rather than five independent coefficients previously thought to prevail. Although it is recognized that the coefficients are functions of time and temperature and stress, it is convenient to abbreviate the functional notation as follows:

$$c_{ij}(t, T, \sigma, \dots) = c_{ij}$$

The stress-strain relationships which result from Equation 3 and 6 are as shown.

$$\begin{aligned} \epsilon_1 &= c_{11} \sigma_1 + c_{12} \sigma_2 + c_{13} \sigma_3 \\ \epsilon_2 &= c_{12} \sigma_1 + c_{11} \sigma_2 + c_{13} \sigma_3 \\ \epsilon_3 &= c_{31} \sigma_1 + c_{31} \sigma_2 + c_{33} \sigma_3 \\ \epsilon_4 &= c_{44} \sigma_4 \\ \epsilon_5 &= c_{44} \sigma_5 \\ \epsilon_6 &= 2(c_{11}-c_{12})\sigma_6 \end{aligned} \quad (7)$$

For uniaxial tension or compression tests in which only  $\sigma_1$  acts, it is found that



$$\begin{aligned}
c_{11} &= \frac{1}{E_1} \\
c_{12} &= \frac{\mu_{21}}{E_1} \\
c_{31} &= \frac{\mu_{31}}{E_1}
\end{aligned} \tag{8}$$

where  $\mu_{ij}$  = Poisson's ratio =  $\frac{\epsilon_i}{\epsilon_j}$  when  $\sigma_j$  is acting,

$$E_i = \frac{\sigma_i}{\epsilon_i} = \text{stiffness when } \sigma_i \text{ is acting } (i = 1, 2, 3)$$

When  $\sigma_3$  acts,  $c_{13}$  and  $c_{33}$  are found to be

$$\begin{aligned}
c_{13} &= \frac{\mu_{13}}{E_3} = \frac{\mu_{23}}{E_3} \\
c_{33} &= \frac{1}{E_3}
\end{aligned} \tag{9}$$

When  $\sigma_4$  or  $\sigma_5$  act the following relations are found

$$c_{44} = c_{55} = \frac{1}{G_4} = \frac{1}{G_5} \tag{10}$$

where  $G_i = \frac{\sigma_i}{\epsilon_i} (i = 4, 5)$

The final form of the stress-strain equations, obtained by substituting Equations 8, 9, and 10 into Equation 7 is as follows:

$$\begin{aligned}
\epsilon_1 &= \frac{1}{E_1} \sigma_1 + \frac{\mu_{21}}{E_1} \sigma_2 + \frac{\mu_{13}}{E_3} \sigma_3 \\
\epsilon_2 &= \frac{\mu_{21}}{E_1} \sigma_1 + \frac{1}{E_1} \sigma_2 + \frac{\mu_{13}}{E_3} \sigma_3 \\
\epsilon_3 &= \frac{\mu_{31}}{E_1} \sigma_1 + \frac{\mu_{31}}{E_1} \sigma_2 + \frac{1}{E_3} \sigma_3
\end{aligned} \tag{11}$$

$$\epsilon_4 = \frac{1}{G_4} \sigma_4$$

$$\epsilon_5 = \frac{1}{G_4} \sigma_5$$

$$\epsilon_6 = \frac{2}{E_1} (1 - \mu_{21}) \sigma_6$$

For small strain, the following relations can be shown to hold. To obtain their magnitudes, it is necessary that volume changes be measured during testing.

$$\mu_{13} = \frac{\Delta V}{2V\epsilon_3} - \frac{1}{2} \quad (12)$$

$$\mu_{21} + \mu_{31} = \frac{\Delta V}{V\epsilon_1} - 1$$

The value of Poisson's ratio,  $\mu_{21}$ , can be found from the results of a uniaxial tension or compression test and a shear test as follows:

$$\mu_{21} = \frac{-E_1}{2G_{13}} + 1$$

For an isotropic, elastic, incompressible material  $G = E/3$  and hence,

$$\mu_{13} = \mu_{21} = \mu_{31} = -\frac{1}{2}$$

which is seen to be a special case of the theory presented here.

It should be noted that the ratio  $E_3/E_1$  might be used as a measure of the anisotropy exhibited by the mixture.

## EXPERIMENTAL INVESTIGATIONS

The laboratory tests described in this section were performed to evaluate the theory of material behavior introduced in the preceding section. Testing procedures were selected that could be used to investigate the stress-deformation behavior of mixtures compacted in the laboratory as well as those placed as pavements in service. Although the results were obtained from laboratory-compacted specimens, similar test procedures could be used to evaluate specimens obtained from highway pavements.

In an attempt to simulate loading conditions that are considered among the most severe encountered in service, the loads applied to test specimens were taken as static loads and were applied for a period of 30 seconds. It was thought that this would be representative of the duration of load that might be expected at signalized intersections where rutting and shoving sometimes occur.

A summary of the material coefficients and the tests used to determine the value of the coefficients is given in Table 1.

Table 1. Summary of Tests

Coefficient	Defining Test
	Type of Test, Load Axis
$C_{11}$	tension, $x_1$ ; compression, $x_1^*$ .
$C_{12}$	tension, $x_1$ ; compression, $x_1^*$ ; volume change, $x_1^*$
$C_{13}$	tension, $x_3$ ; compression, $x_3^*$ ; volume change, $x_3^*$
$C_{31}$	tension, $x_1$ ; compression, $x_1^*$ ; volume change, $x_1^*$
$C_{33}$	tension, $x_3$ ; compression, $x_3^*$ ; volume change, $x_3$
$C_{44}$	direct shear, $x_{12}^*$ , torsion, $x_{12}^*$

\* The tests marked with an asterisk are tests used in this study to define the coefficients.

Information on Materials and Preparation of Specimens is presented in the following sections, followed by a presentation of test results. The results of laboratory tests are presented along with comments on trends and relationships indicated by the data. The presentation is organized in the following sequence:

1. Uniaxial Compression Test Results
2. Direct Shear Test Results
3. Comparison of Shear and Torsion Test Results

### Materials and Preparation of Specimens

Specimens for compression, shear and torsion tests were prepared from bituminous mixtures of the same composition. Table 2 shows the sieve analysis and origin of the aggregate used in the bituminous mixture.

The aggregate was blended in 2200 gram batches and then heated to 325°F prior to being mixed with asphalt.

A 60-70 penetration asphalt cement having the properties shown in Table 3 was used in this study. The asphalt was heated to 325°F and then mixed with the heated aggregate in a mechanical mixer for two minutes. The weight of asphalt cement mixed with the aggregate was five percent by weight of the aggregate. After mixing was completed, each batch was put in flat pans and placed in a forced-draft oven to cure for 24 hours at 140°F.

Compaction of the bituminous mixture was started after the mixture was reheated to 325°F. The heated mixture was placed in two layers in the heated beam mold shown in Figure 5. Each layer was tamped 25 times with a 1/2-inch diameter, round-end tamping rod.

The mixture in the beam mold was compacted in the kneading compactor by the special tamping foot shown in the figure. The mixture was compacted with the tamping foot by moving the mold back and forth its entire length under the tamping foot four times, using eight tamps during each one-way traverse, for each of four different compaction pressures. Foot pressures used in compaction were 20, 35, 100 and 120 psi, in that order. After the beam was compacted on its top side according to this procedure, the mold and beam were inverted and the procedure was repeated. Hence, the top and the bottom of the beam received the same compactive effort.

After the beam was compacted, it was removed from the mold and placed in a forced-draft oven and cured for 24 hours at a temperature of 140°F.



TABLE 2  
Sieve Analysis of Aggregates

<u>Sieve</u>		<u>Fraction, %</u>	<u>Material</u>
Passing	Retained		
No. 4	No. 6	17	Crushed Greencastle Limestone
No. 6	No. 8	13	" " "
No. 8	No. 16	20	River Terrace Sand (Lafayette)
No. 16	No. 30	17	" " " "
No. 30	No. 50	13	" " " "
No. 50	No. 100	10	" " " "
No. 100	No. 200	5	" " " "
No. 200		5	Greencastle Limestone Filler

TABLE 3

## Results of Tests on Asphalt Cements

Specific Gravity @ 77°F	1.036
Softening Point, Ring and Ball, °F	124
Ductility at 77°F, 5 cm/min, cm	100+
Penetration, 100 grams, 5 sec., 77°F	66
Penetration, 200 grams, 60 sec., 32°F	17
Loss on Heating, 50 grams, 5 hr., 325°F, %	0.01
Penetration of Residue, percent of original	89
Flash Point, Cleveland Open Cup, °F	595
Solubility in CCl <sub>4</sub> , percent	99.84

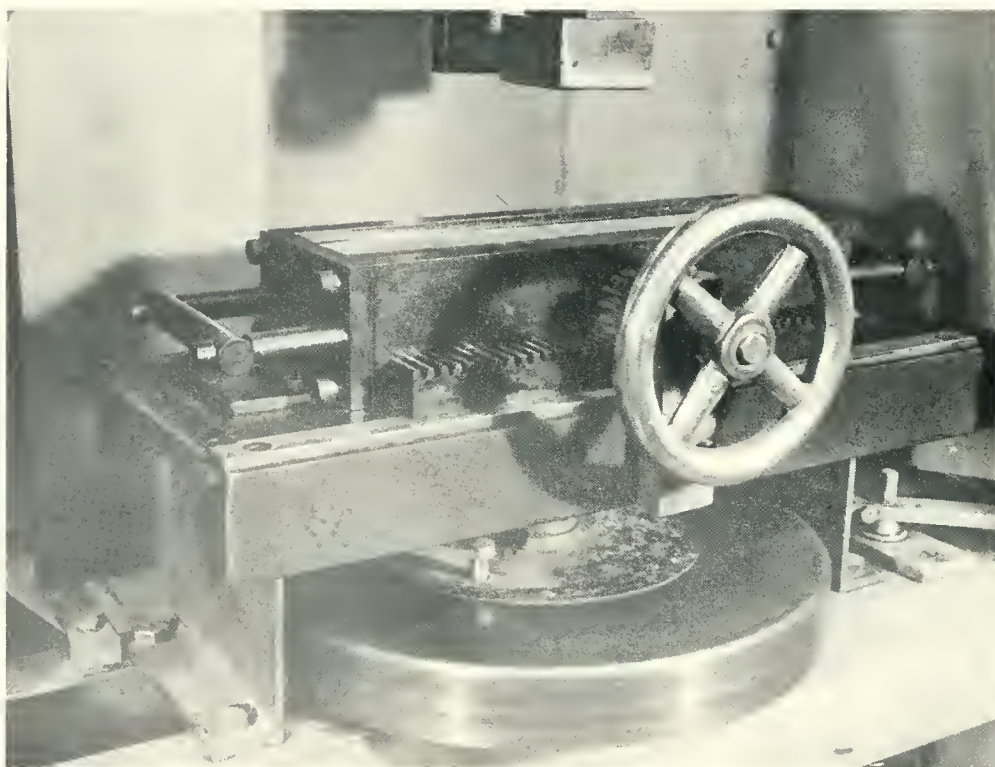


FIGURE 5. MOLD AND TAMPING FOOT FOR  
COMPACTING BEAM OF BITUMINOUS MIXTURE

After the curing period, the beam was cooled to room temperature.

One-inch pieces were cut from both ends of the beams and wasted. This was done because it was recognized that confinement at the ends of the beam mold might cause compaction conditions to be atypical at these locations. The compacted beam was cut into specimens by use of a masonry saw equipped with a diamond blade.

Specimens for uniaxial compression testing were cut approximately 0.05 inch oversize. Final shaping and polishing were accomplished on a lapping wheel using 100 and 800 mesh grinding compounds, respectively. Final dimensions of the compression test specimens were 1 x 1 x 2.05 inches. These dimensions were obtained by utilizing the jig shown in Figure 6 during shaping and polishing.

Specimens for shear testing were also cut oversize from the beam and then ground and polished to test dimension on a lapping wheel. Final dimensions of the shear test specimens were  $1/2 \times 1/2 \times 2-1/8$  inch. The long dimension of the specimen was parallel with the  $x_1$  axis of the beam shown in Figure 24 in the Appendix.

Torsion specimens with an outside diameter of  $1-1/8$  inch were cut from the compacted bituminous mixture and polished on the lapping wheel. The height of the test specimens was  $1/2$  inch. The axis of the cylindrical torsion specimens was parallel with the  $x_3$  axis of the compacted beam.

After the specimens were polished, they were secured to the specimen holders shown in Figures 7 and 8 by an epoxy. When the epoxy had hardened, the specimens were placed in a constant temperature room for at least four hours prior to testing. Each specimen was tested on the test stand shown in the foreground of Figure 9. Compression and shear specimens were bolted to the steel plate fixed on the surface of the test stand while the torsion specimens were tested on the frame over the concrete base. Test loads were

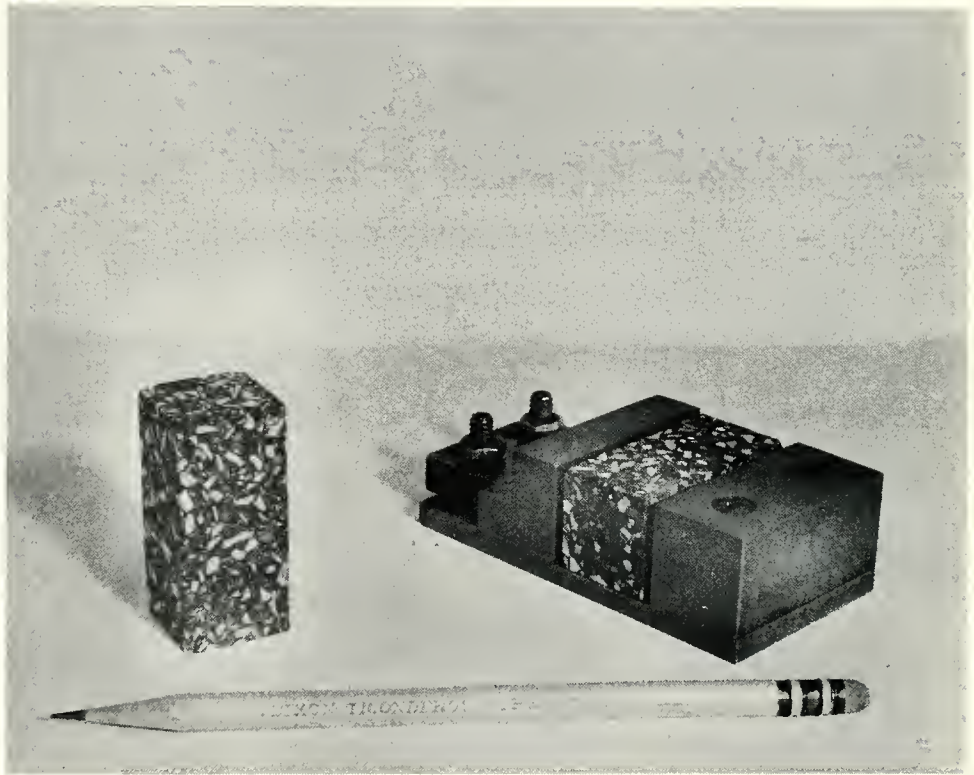


**FIGURE 6. UNIAXIAL COMPRESSION SPECIMENS  
WITH JIG FOR SIZING**



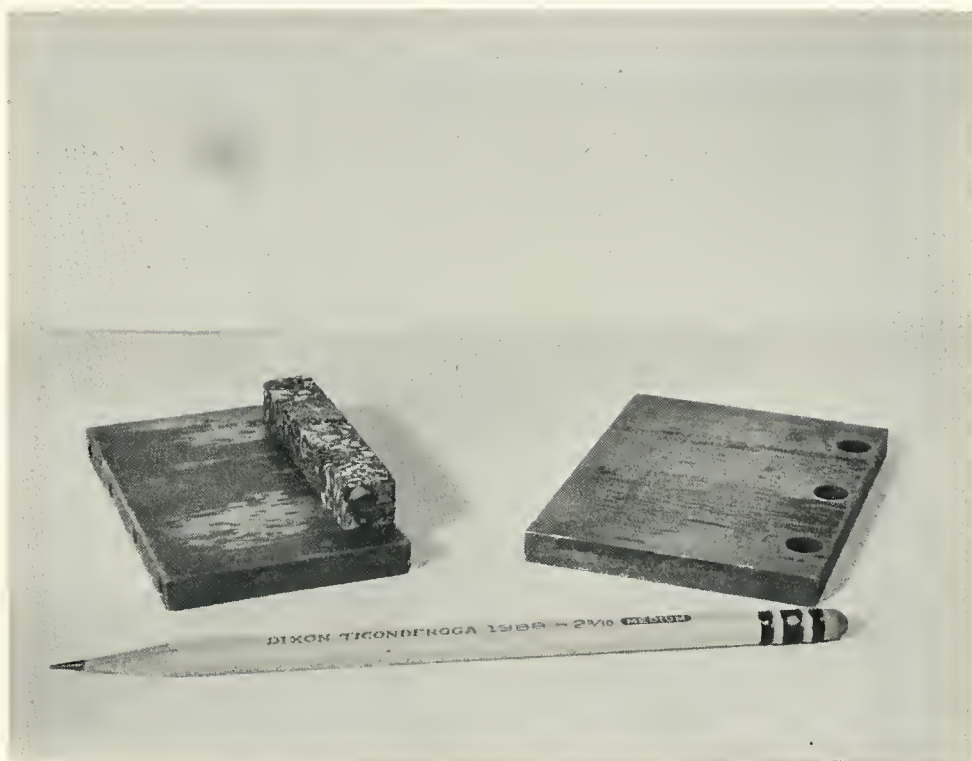
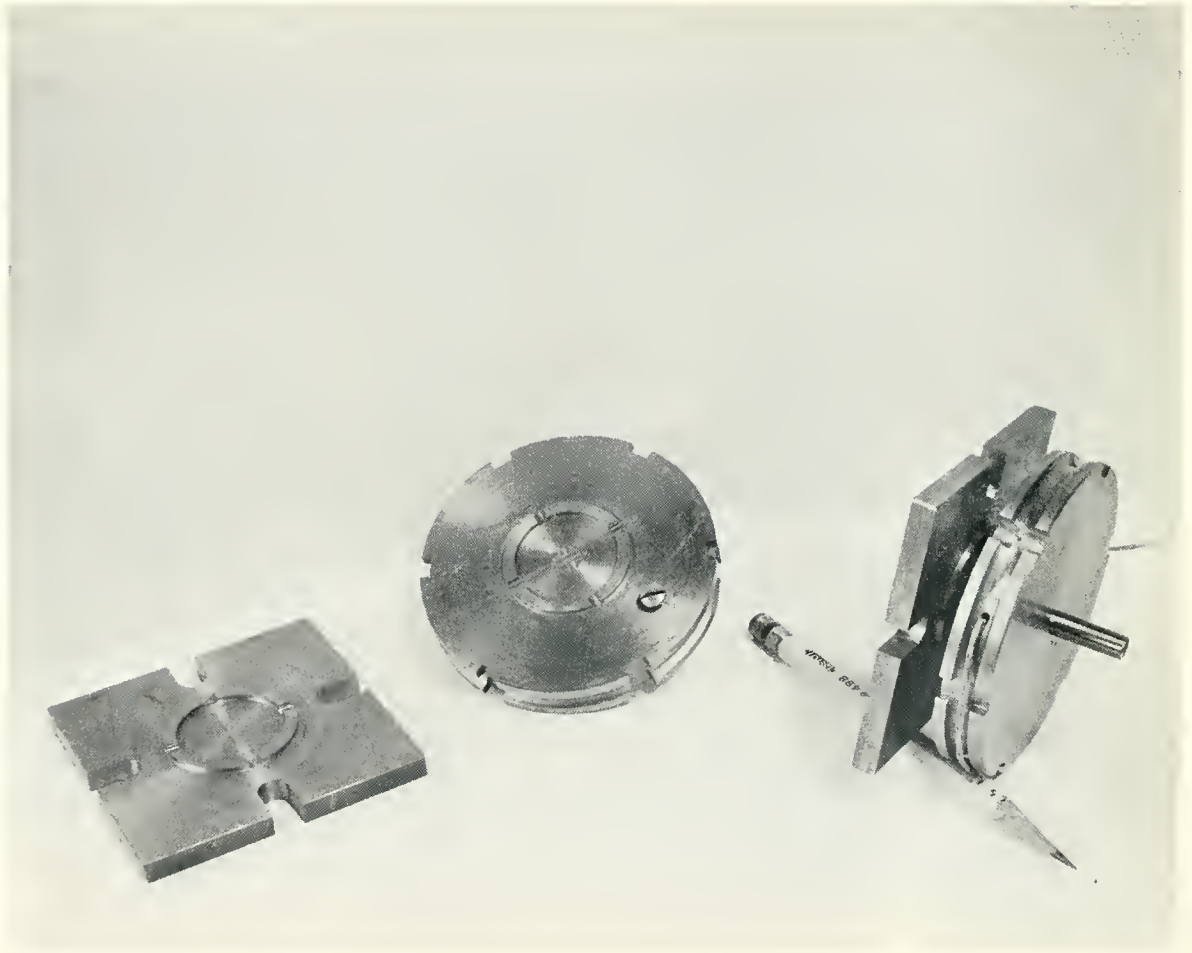
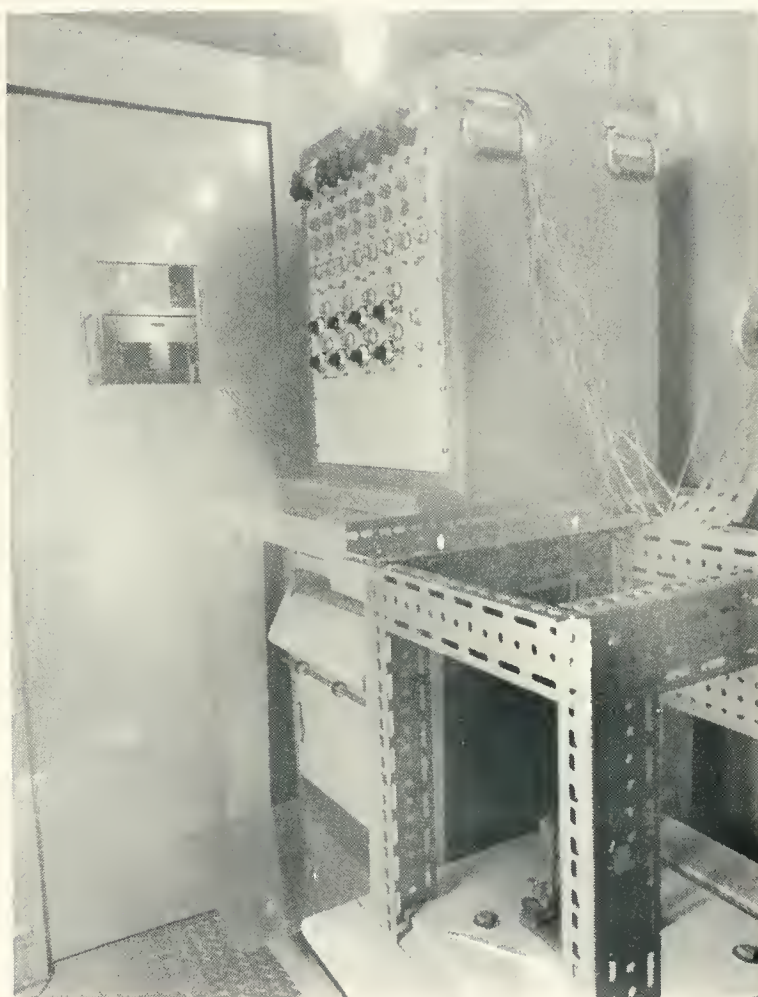


FIGURE 7. DIRECT SHEAR SPECIMEN  
AND SPECIMEN HOLDER



**FIGURE 8. TORSION SPECIMEN HOLDERS**



**FIGURE 9. INTERIOR OF CONSTANT TEMPERATURE ROOM SHOWING TEST STAND AND RECORDER**

applied for 30 seconds and load magnitudes were 23.1, 40.8 and 58.3 psi, respectively. Tests loads for shear (Figure 7) and torsion testing (Figure 10) were applied by lead weights acting through a wire and pulley arrangement. Compression loads were applied by lead weights resting on a shaft that was seated on the spherical bearing piece shown in Figure 11. The three stresses were applied to specimens at temperatures of 70, 80 and 90°F. An electronic recorder and strain gage displacement transducers like that shown in Figure 12 were used to obtain data records as shown in Figure 13.

### Uniaxial Compression Test Results

Data from uniaxial compression tests are plotted in Figure 14. Plots of these data for specimens obtained from the same compacted beam are shown in the upper portion of Figure 14. Data indicate that the stiffness moduli,  $E_1$  and  $E_3$ , vary linearly with time on a log-modulus vs. log-time plot. Data are presented for uniaxial tests along both the  $x_1$  and  $x_3$  axes and for test temperatures of 70, 80 and 90°F.

The numbers on each curve in Figure 14 are least square slopes computed on an electronic computer. In all cases, the slopes of the lines are negative and hence mixture stiffness, as defined by  $E_1$  and  $E_3$ , decreases with time. The trend of behavior indicates that the moduli determined from compression tests decrease with increases in temperature.

It was anticipated that data for time values of less than five seconds might yield relations similar to those shown; however, experimental error was considered excessive for loading times less than five seconds. Error was introduced, in part, by deviations in placing the load on the specimen and uncertainty in interpreting from the graphic data where the initial time,  $t = 0$ , was located. Initial seating of the load and inertia effects



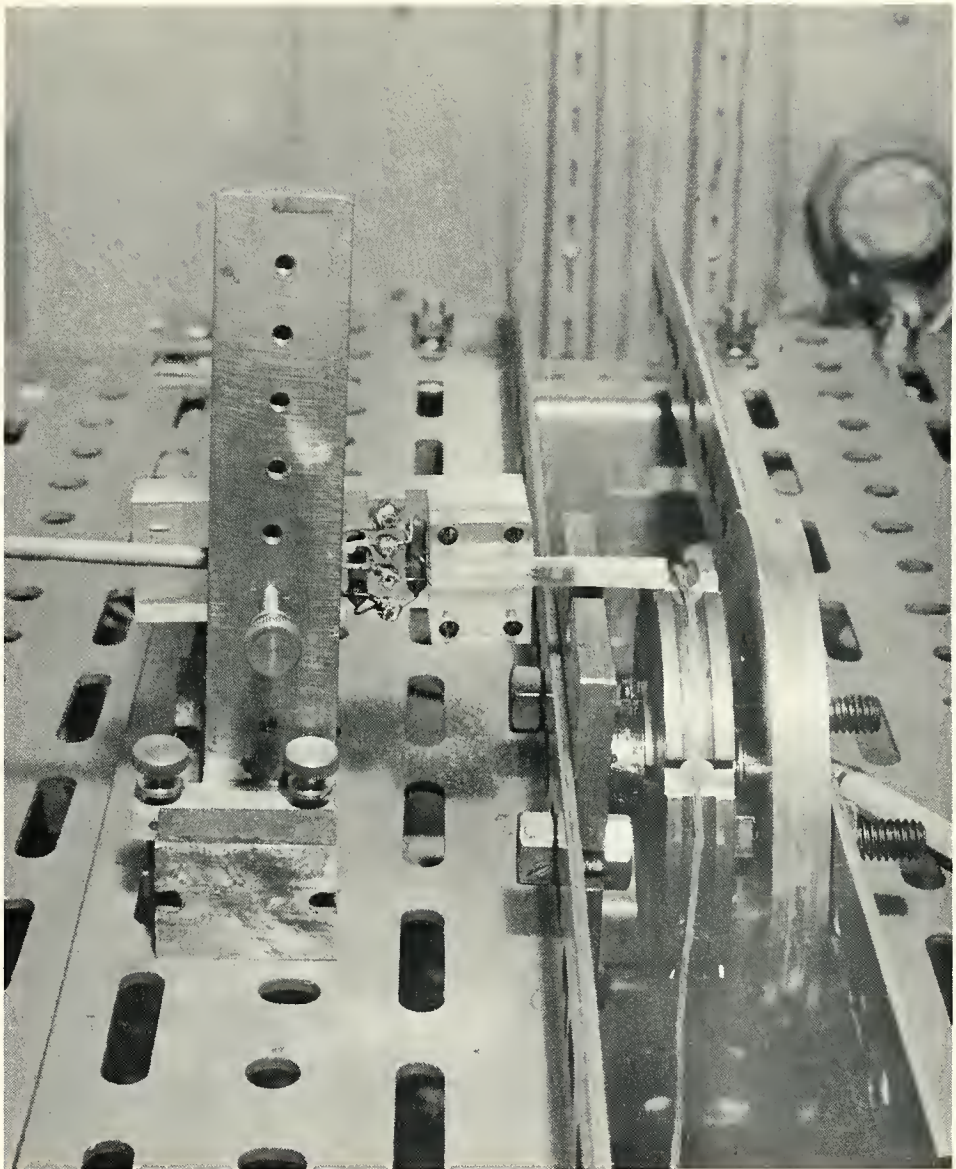


**FIGURE 10. TORSION SPECIMEN AND  
DISPLACEMENT TRANSDUCER**

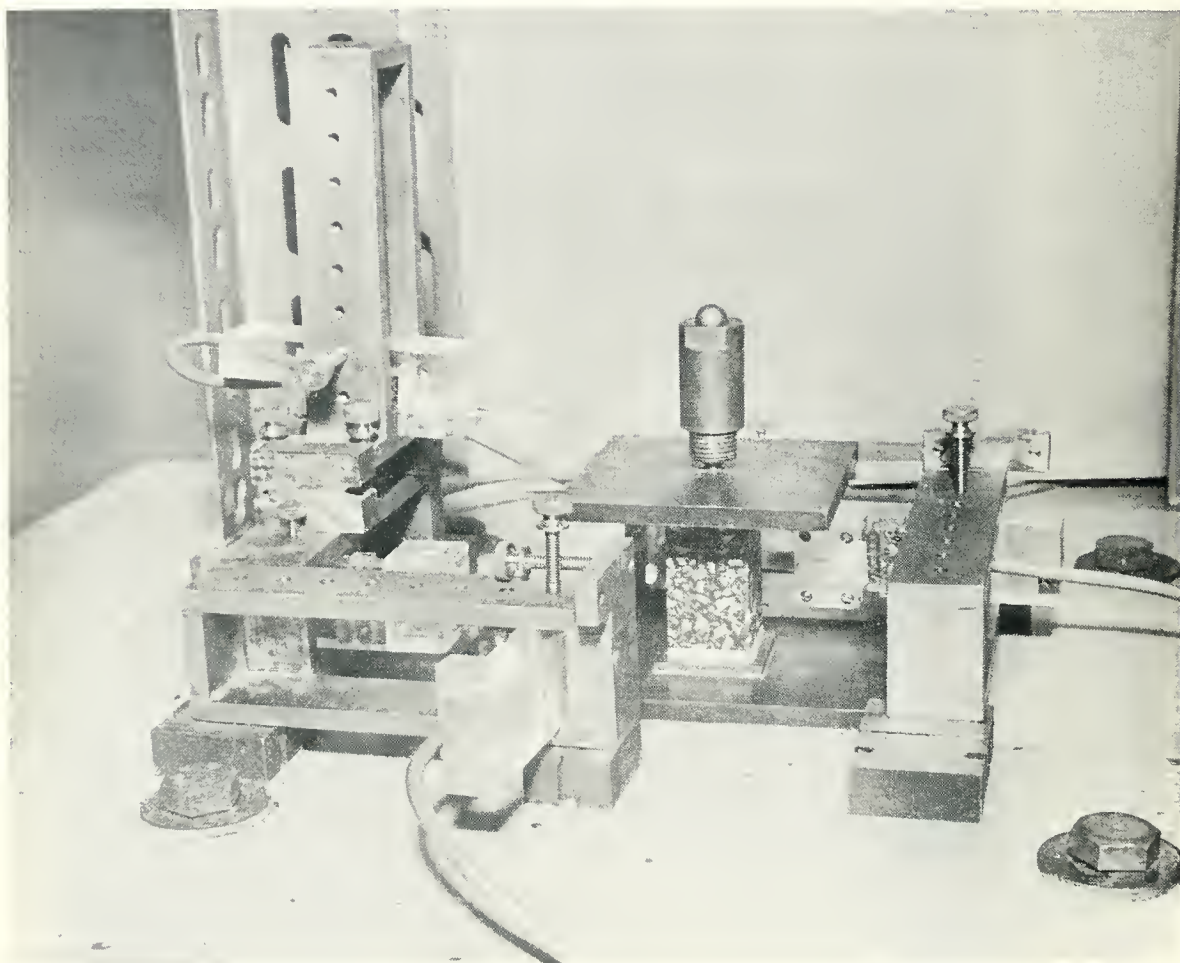


FIGURE II.      UNIAXIAL COMPRESSION  
SPECIMEN WITH TRANSDUCERS  
AND HOLDERS





FIGURE 12. DISPLACEMENT TRANSDUCER

SPECIMEN: DIRECT SHEAR  
 STRESS:  $\sigma_{12} = 40.8 \text{ psi}$   
 CHART SPEED: 0.5 cm/sec  
 POWER AMPLIFIER: X .02  
 PREAMPLIFIER: 5 mv/cm  
 TEMPERATURE: 70°F

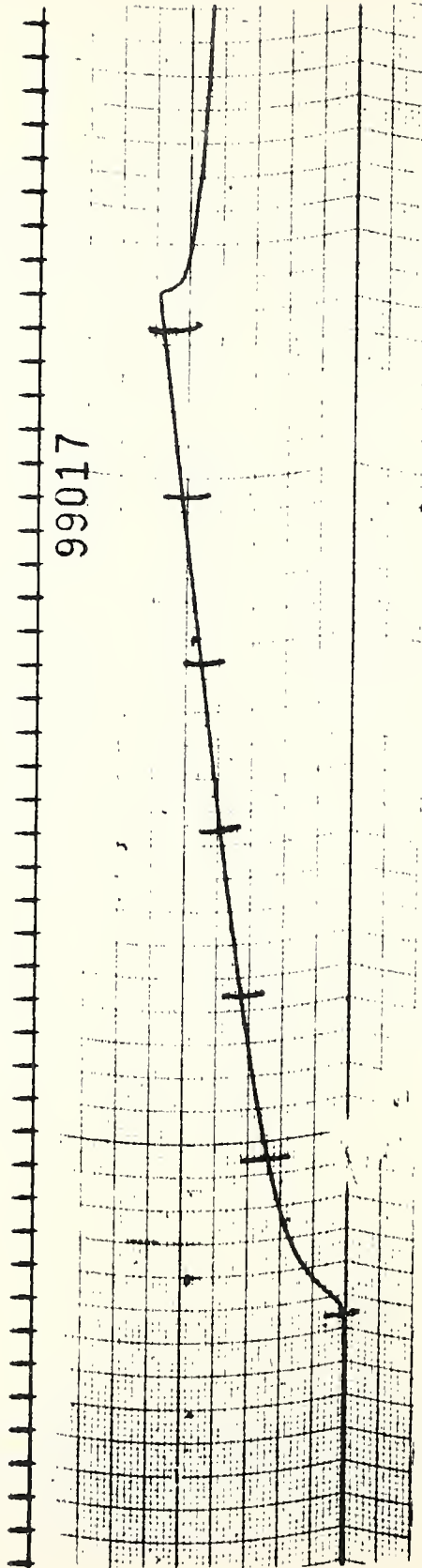


FIGURE 13. TYPICAL GRAPHICAL DATA FOR  
 COMPRESSION, SHEAR AND TORSION TESTS

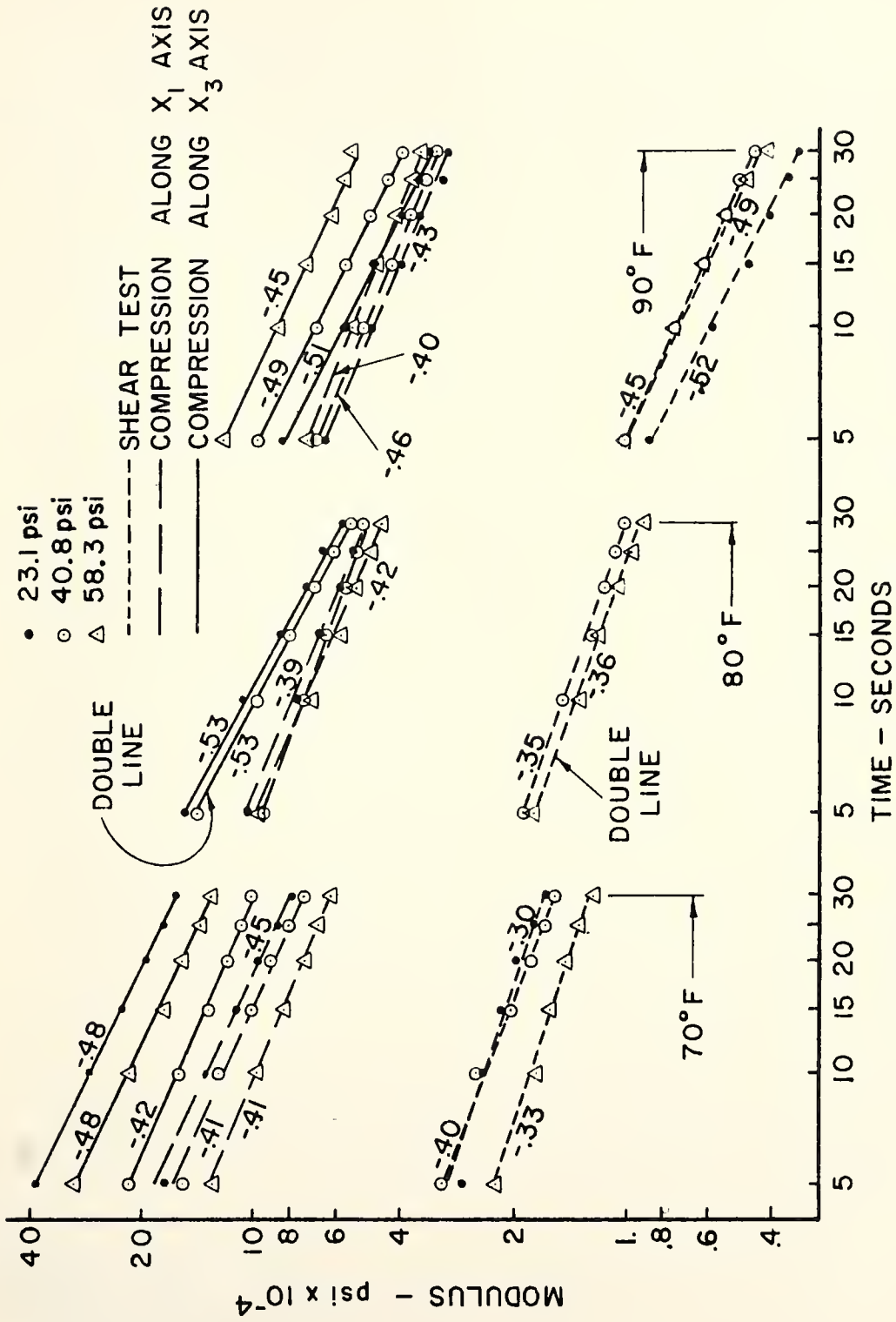


FIGURE 14. COMPRESSION AND SHEAR MODULI VS. TIME, 70°, 80°, 90°F

at small values of time would also add to erroneous determination of stiffness for small strains.

Although plots of the log-modulus vs. log-time appeared linear, several coefficients of linear correlation were computed to obtain a measure of how well the data could be approximated by a straight line. All the linear correlation coefficients were greater than 0.95 and most were very close to 1.0. Linearity on a log-log plot, based on the magnitude of the correlation coefficients, assists description of material behavior.

A measure of the anisotropy of the mixture tested is given by the ratio  $E_3/E_1$ . Figure 15 shows plots of this ratio obtained from data of Figure 14. It should be noted from this figure that for the highest stress level and for all three test temperatures used in this study, anisotropy is essentially constant over the time range considered. The data indicate that anisotropy exists for laboratory-compacted specimens, at least for some mixtures. Behavior of a similar nature may be expected to be present in field-compacted mixtures. In all cases shown in Figure 15 the value of  $E_3$  is greater than  $E_1$  and the ratio  $E_3/E_1$  for all data of Figure 15 has the approximate range 1.8 to 1.1. From this it can be noted that the mixture is stiffer in the direction of applied compactive forces than it is in orthogonal directions.

Poisson's ratio is defined as (transverse strain) / (longitudinal strain). Values of this ratio were necessary for the determination of the material coefficients,  $C_{12}$ ,  $C_{13}$ , and  $C_{31}$ ; hence, plots of transverse strain vs. longitudinal strain were made from data obtained from uniaxial compression tests. Poisson's ratio is the slope of these curves. Several coefficients of linear correlation were computed to obtain a measure of

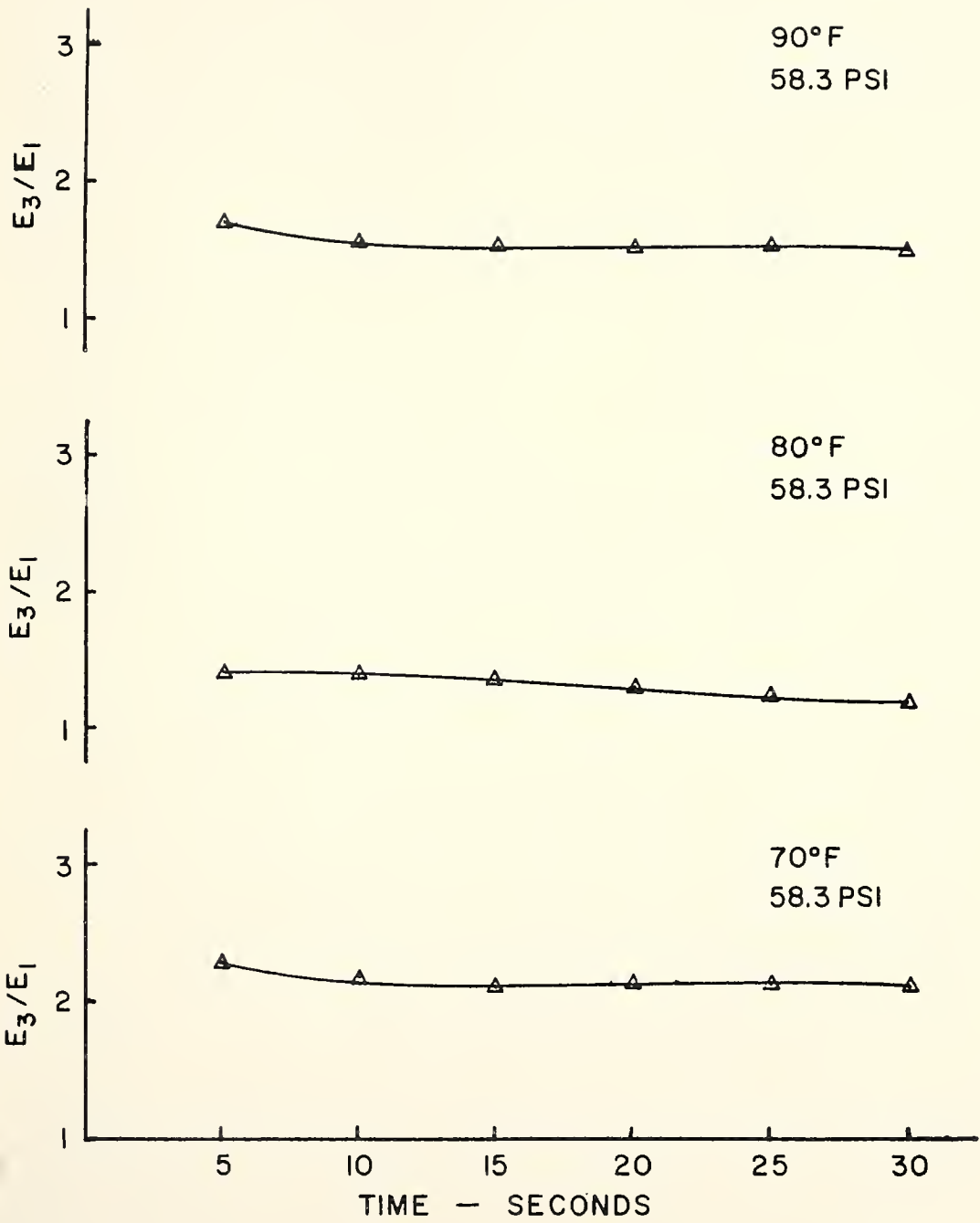


FIGURE 15.  $E_3/E_1$  VS. TIME

the linearity of Poisson's ratios for the loading conditions utilized in this research. The data indicated that Poisson's ratio was constant for the duration of loading considered. Representative plots of transverse strain vs. longitudinal are shown in Figure 16.

Efforts to obtain the values of Poisson's ratios by inspection were found to be inaccurate and hence a least squares slope was calculated for each of the specimens by use of a computer program. A tabulation of some values of Poisson's ratios determined from uniaxial compression tests is shown in Table 4.

It can be noted from the data that the values of Poisson's ratio were erratic. It was hypothesized that the particulate nature of the material being tested was responsible for this erratic measurement. Volume change measurements were made to obtain an average value that would not be so dependent on the behavior of individual aggregate particles.

Results from uniaxial compression tests with volume change measurements are presented in Tables 5 and 6. Figure 17 shows graphically the data from Tables 5 and 6 when Poisson's ratios are plotted as functions of time. The specimens used in these tests were prepared from the same beam and from the same orientations as the specimens tested in uniaxial compression tests without volume change measurements.

Data presented graphically indicate Poisson's ratios are slowly varying functions of time of loading for the time interval of one hour. For short durations of load the assumption that Poisson's ratio does not vary appears to be justified. Poisson's ratio varies in these particular tests from approximately 0.43 to 0.52.

The determination of Poisson's ratios by volume change measurements appears to be a satisfactory mode of measurement although extrapolation to smaller time values is presently required. The smallest value of



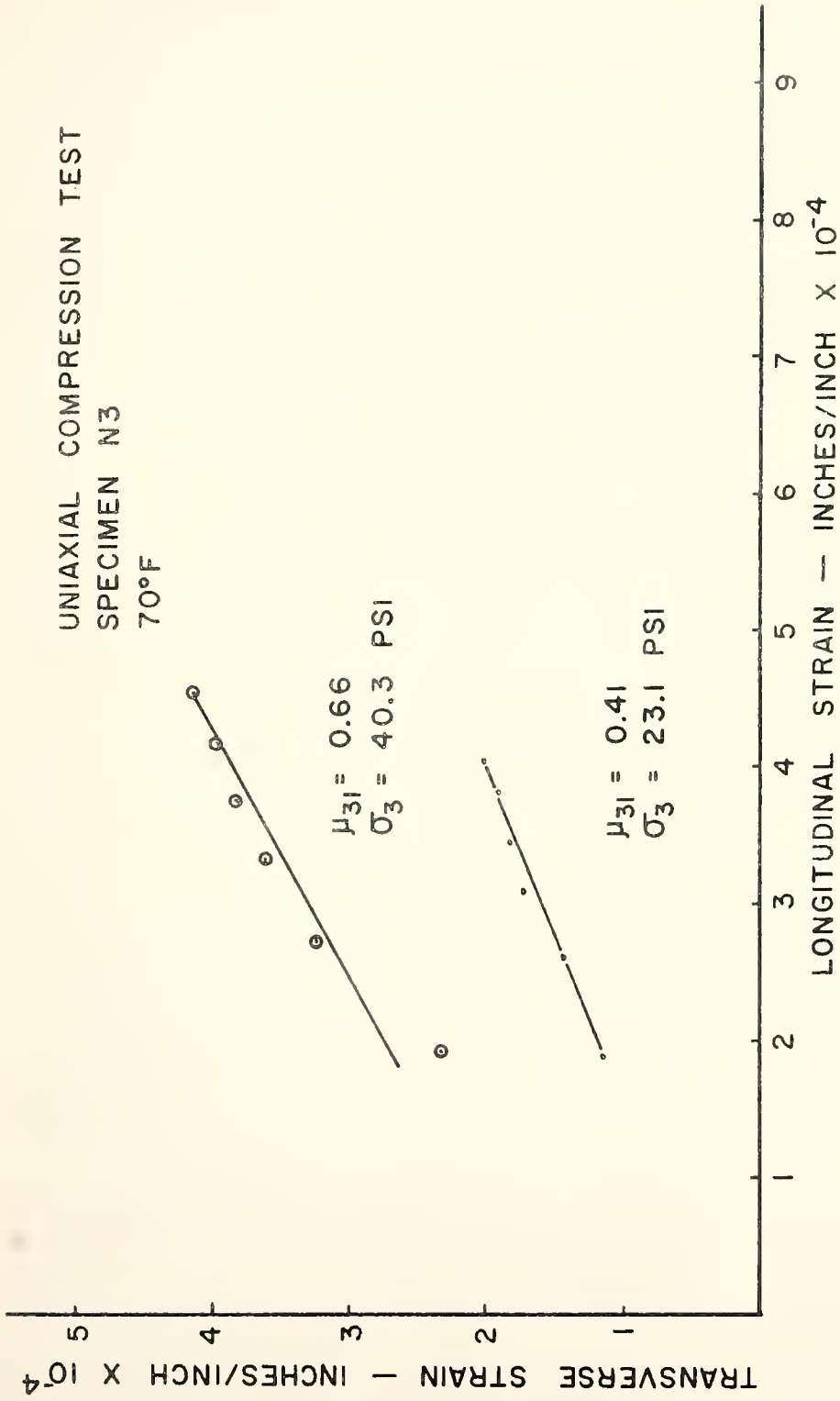


FIGURE 16. TRANSVERSE STRAIN VS. LONGITUDINAL STRAIN  
AND SLOPES DEFINING POISSON'S RATIO

TABLE 4

Poisson's Ratios Obtained from Uniaxial Compression

Test Temperature: 80°F

<u>Stress, psi</u>	<u>(-) <math>\mu_{21}</math></u>	<u>(-) <math>\mu_{31}</math></u>
23.1	1.33	0.21
	0.25	0.45
	0.48	0.40
	0.44	0.24
	0.66	0.47
	1.26	0.27
	0.31	
40.8	0.47	0.28
	0.47	0.43
	0.40	0.59
	0.46	0.31
	0.42	0.81
	0.68	0.33
	0.42	0.50
	0.63	0.37
	0.52	
58.3	0.45	0.40
	0.41	0.25
	0.30	0.50
	0.27	0.34
	0.78	0.79
	0.38	0.35

TABLE 5

Poisson's Ratio,  $\mu_{13}$ 

Obtained from Uniaxial Compression Test with Volume Change Measurement

Specimen N3

95°F, 61.7 psi

Volume = V = 33.6 cc

Length =  $L_3$  = 5.2 cm

Time (min)	$\Delta V$ (cc)	$\Delta L_3$ (cm)	$\frac{\Delta V L_3}{2V \Delta L_3}$	$\mu_{13} = \frac{\Delta V L_3}{2V \Delta L_3} - \frac{1}{2}$
1	-0.0323	-0.0355	0.0704	-0.43
5	-0.0323	-0.0559	0.0464	-0.45
10	-0.0337	-0.0686	0.0380	-0.46
15	-0.0294	-0.0762	0.0298	-0.47
20	-0.0264	-0.0826	0.0247	-0.48
25	-0.0230	-0.0890	0.0199	-0.48
30	-0.0149	-0.0915	0.0126	-0.49
35	-0.0109	-0.0978	0.0086	-0.49
40	-0.0067	-0.1017	0.0051	-0.49
45	-0.0011	-0.1054	0.0005	-0.50
50	0.0022	-0.1092	-0.0016	-0.50
55	0.0055	-0.1130	-0.0038	-0.50
60	0.0110	-0.1169	-0.0094	-0.51

TABLE 6

Poisson's Ratios,  $\mu_{21} + \mu_{31}$ 

Obtained from Uniaxial Compression Test with Volume Change Measurement

Specimen N1  
 95° F, 61.7 psi  
 Volume = V = 33.6 cc  
 Length =  $L_1$  = 5.2 cm

Time (min)	$\Delta V$ (cc)	$\Delta L_1$ (cm)	$\frac{\Delta V L_1}{V \Delta L_1}$	$\mu_{21} + \mu_{31} = \frac{\Delta V L_1}{V \Delta L_1} - 1$
1	-0.0165	-0.0216	0.1182	-0.8818
5	-0.0209	-0.0484	0.0668	-0.9332
10	-0.0136	-0.0585	0.0360	-0.9640
20	0.0003	-0.0712	-0.0010	-1.0010
25	0.0105	-0.0763	-0.0212	-1.0212
30	0.0114	-0.0827	-0.0214	-1.0214
35	0.0161	-0.0877	-0.0284	-1.0284
40	0.0196	-0.0915	-0.0332	-1.0332
45	0.0210	-0.0978	-0.0332	-1.0332
50	0.0216	-0.0940	-0.0322	-1.0322
55	0.0275	-0.1079	-0.0394	-1.0394
60	0.0370	-0.1105	-0.0518	-1.0518

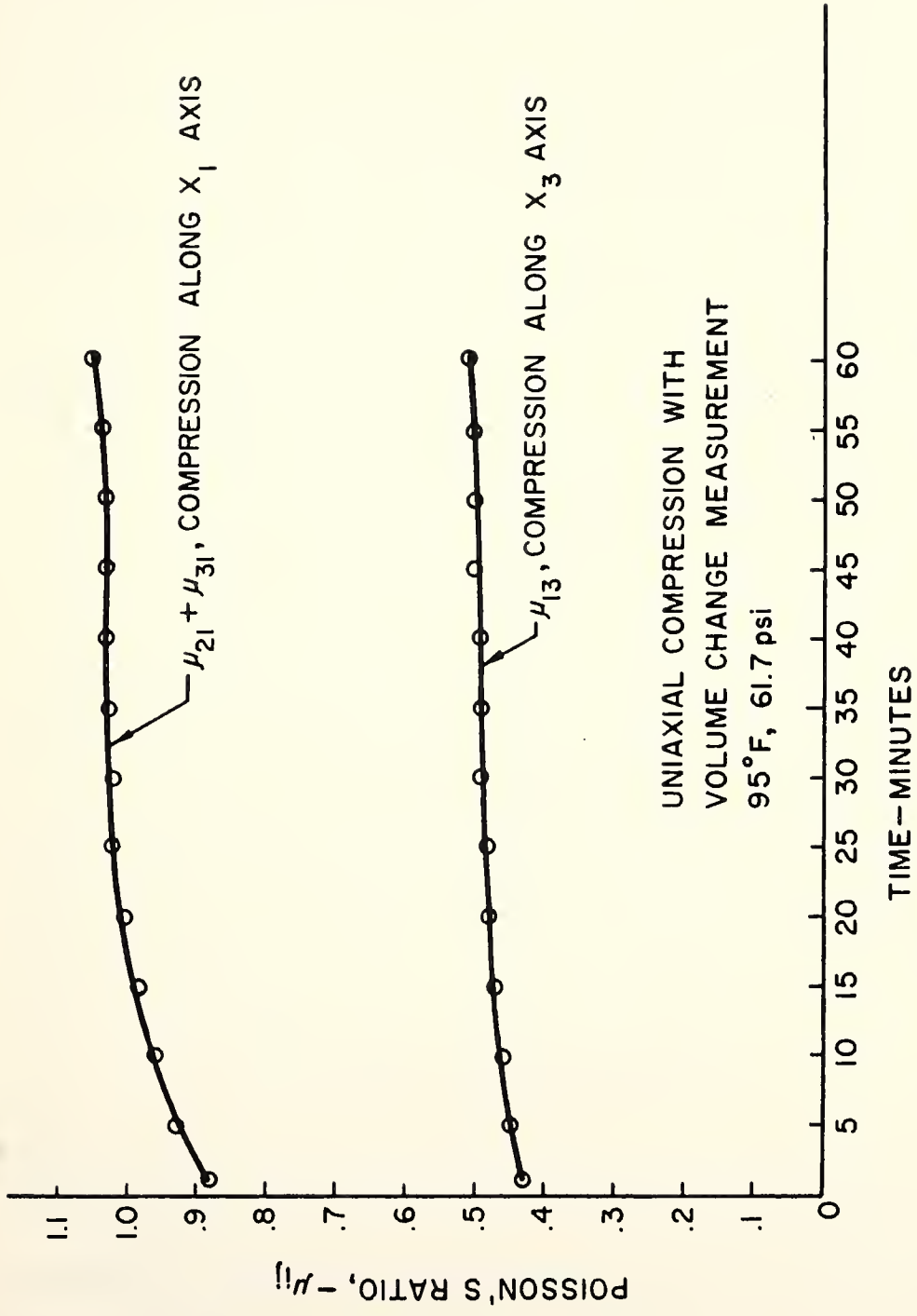


FIGURE 17. POISSON'S RATIO VS TIME FROM  
VOLUME CHANGE MEASUREMENTS

Poisson's ratio in the tabular data was selected as that most representative of the ratio that existed during shorter loading times. Hence, the value of  $\mu_{13}$  was -0.43 as shown after the one minute reading in Table 5.

The sum of  $\mu_{21}$  and  $\mu_{31}$  can be determined by considering some relations obtained from volume change measurements.

The volume dilation expressed as a function of strain invariants is:

$$\frac{\Delta V}{V} = \sqrt{1 + 2J_1 - 4J_2 + 8J_3} - 1$$

where  $J_1$ ,  $J_2$  and  $J_3$  are the first, second and third invariants of strain, respectively. For small strains this expression reduces to:

$$\frac{\Delta V}{V} = \sigma_1 (C_{11} + C_{12} + C_{31})$$

or

$$\frac{\Delta V}{V \epsilon_1} - 1 = \mu_{21} + \mu_{31} = \frac{\epsilon_2}{\epsilon_1} + \frac{\epsilon_3}{\epsilon_1}$$

From Figure 15 it can be noted that the degree of anisotropy can be characterized by the ratio  $E_3/E_1$ . It appears that a representative value of this quantity might be in the range 1.1 to 1.8. If 1.5 is selected as a representative value of this ratio for the duration of loads and the range of temperature investigated, then

$$E_3 = 1.5E_1 \quad \text{and}$$

$$E_3 = 1.5E_2 \quad \text{for transverse anisotropy.}$$

In the absence of other relationships it was assumed that the strain ratio  $\epsilon_3/\epsilon_2$ , which involves strains in directions orthogonal to the applied stress, could be approximated by  $E_2/E_3$ . Hence,

$$\frac{\Delta V}{V \epsilon_1} - 1 = \frac{\epsilon_2}{\epsilon_1} + \frac{\epsilon_3}{\epsilon_1}$$



may be written  $\frac{\Delta V}{V\epsilon_1} - 1 = \frac{1.5\epsilon_3 + \epsilon_3}{\epsilon_1} = 2.5\mu_{31}$

From Table 5 it is found that after one minute

$$\frac{\Delta V}{V\epsilon_1} - 1 = -0.88$$

hence

$$2.5\mu_{31} = -0.88$$

$$\mu_{31} = -0.35$$

$$\mu_{21} = -0.53$$

From the two compression tests, five of the six material coefficients for transverse anisotropy have been determined. Writing these coefficients in functional notation gives:

$$C_{11}(t, T, \sigma) = \frac{1}{E_1(t, T, \sigma)}$$

$$C_{33}(t, T, \sigma) = \frac{1}{E_3(t, T, \sigma)}$$

$$C_{12}(t, T, \sigma) = \frac{-0.53}{E_1(t, T, \sigma)}$$

$$C_{31}(t, T, \sigma) = \frac{-0.43}{E_1(t, T, \sigma)}$$

$$C_{13}(t, T, \sigma) = \frac{-0.35}{E_3(t, T, \sigma)}$$

Because Poisson's ratio varies slowly over a relatively long time interval in testing, these ratios are assumed to be constant for the material. Because the stiffness moduli,  $E_1$  and  $E_3$ , are characterized by the logarithmic slope,  $m$ , and the 30 second intercept,  $E_1$  may be written:

$$\log E_1(t, T, \sigma) = \log E_1(30, T, \sigma) + m(t, T, \sigma) \log t$$

A similar expression holds for the modulus  $E_3$ .

#### Direct Shear Test Results

Shear test results from specimens cut from the same beam of compacted bituminous material are shown in the lower portion of Figure 14. The results show that the moduli defined from shear tests behave in approximately the same way as the moduli determined from compression tests.

Hence the shear modulus has the form:

$$\log G_{13}(t, T, \sigma) = \log G_{13}(30, T, \sigma) + m'(t, T, \sigma) \log t$$

where, as in the preceding section, the quantities  $G_{13}(30, T, \sigma)$  and  $m'(t, T, \sigma)$  characterize the deformation response of the mixture to specific inputs.

In all cases, shear test moduli are less than compression moduli. Some questions arose concerning the appropriate thickness of test specimens for obtaining shear without bending. The criterion for selecting 1/2-inch thick specimens was that this thickness permitted the least interference of boundary conditions with the maximum size particles since smaller thicknesses would not be at least two multiples of the nominal maximum size aggregate. Specimens of 1/4-inch thickness were also tested in direct shear and results for some of these tests are shown in Figures 18 and 19. Because the thinner test specimens yielded an increase of the moduli of only several percent rather than a many-fold increase, it was decided that bending influences were minimal in the 1/2-inch thick specimen and hence this specimen size was satisfactory for the determination of shear moduli.

From Figure 14 it can be seen that the slopes of the compression moduli and the shear moduli are approximately equal. This implies that the ratio  $E/2G_{13}$  and  $1 - \mu_{21}$  will be constant over the time range considered here. This is also an indication of the independence of Poisson's ratio with respect to time of loading.

#### Comparison of Shear and Torsion Test Results

Comparison of shear moduli obtained from tests with different boundary conditions was required to determine whether a necessary condition for the invariance of material coefficients was satisfied. Monismith et al

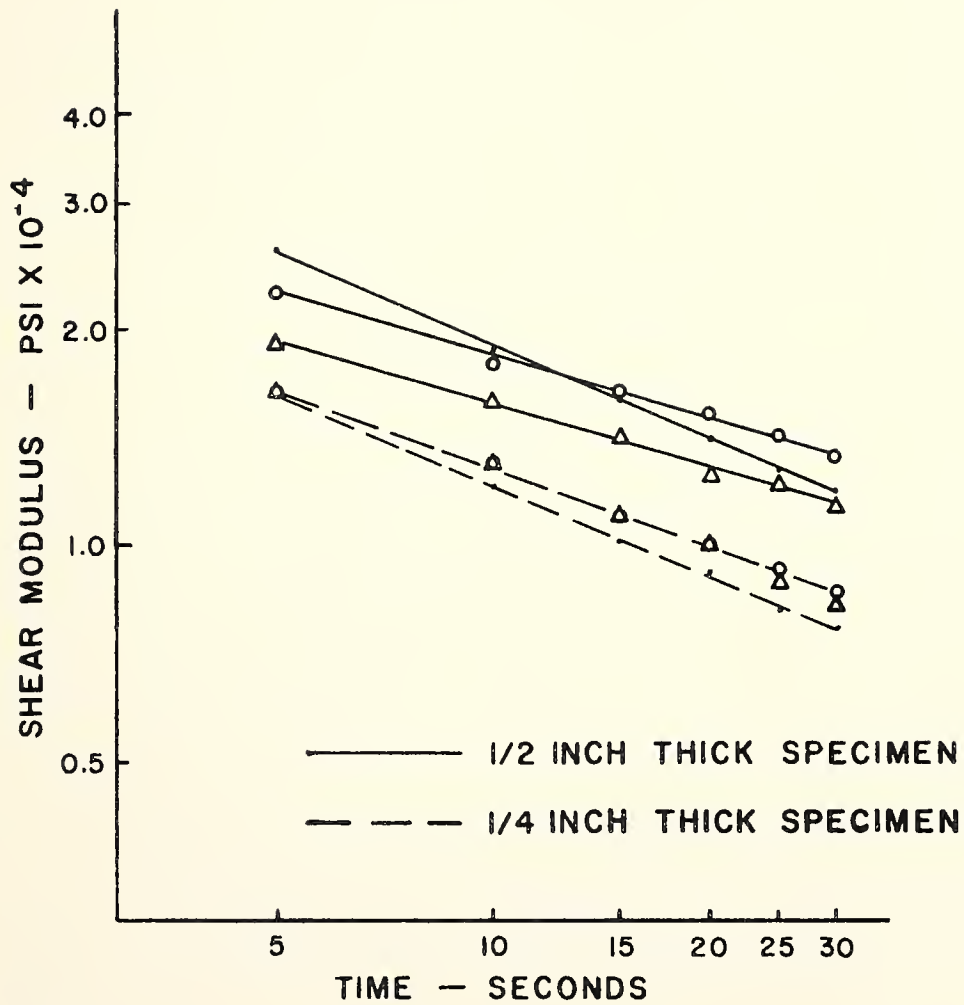


FIGURE 18. SHEAR MODULUS VS. TIME, 80°F

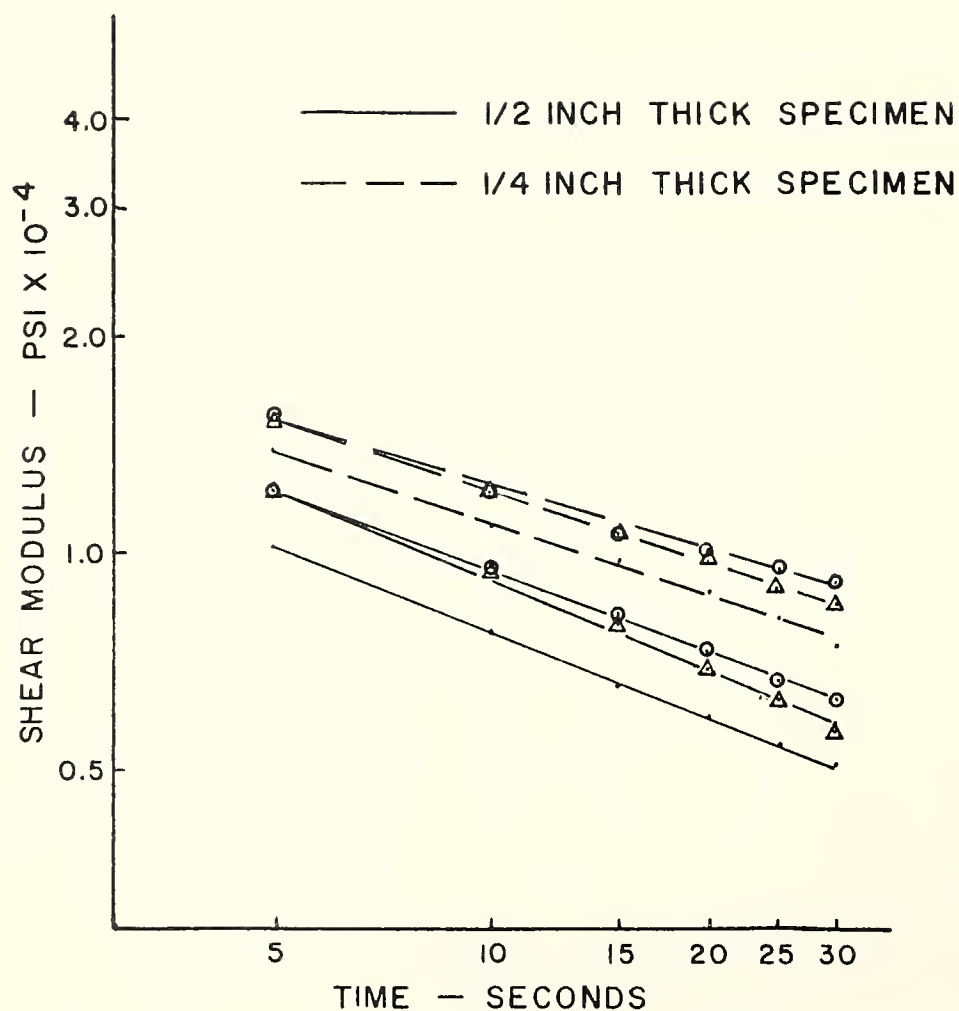


FIGURE 19. SHEAR MODULUS VS. TIME, 90°F

(18) presented creep data obtained from both tension and compression tests at 40°F and noted that strains were invariant for the two tests for axial stresses of 77 psi and axial strains of approximately 0.1 percent. By utilizing several different tests, Lal (10) determined invariant properties of a sheet asphalt mixture.

Six specimens for direct shear testing and six specimens for torsion testing were cut from the same beam of compacted bituminous mixture. The volumes and loaded areas of the specimens tested in direct shear and torsion were as follows:

	Direct Shear	Torsion
Volume of Material, in <sup>3</sup>	0.53	0.50
Loaded Area, in <sup>2</sup>	1.06	0.98

It should be noted that the volumes and loaded areas of the test specimens are nearly equal. Results of tests are presented in Tables 7 and 8 and in Figures 20, 21, and 22. The logarithmic slopes and intercepts at 30 seconds of loading for each stress are presented in Tables 7 and 8. Ninety-five percent confidence intervals are plotted in Figures 20, 21, and 22 and show that the two tests with different boundary conditions yield essentially the same value for the moduli even though experimental deviations exist for results from each test. Consequently, it can be concluded that the values of the moduli obtained are invariant material coefficients.

The area of the two overlapping confidence intervals is shaded in Figures 20, 21, and 22. This overlap further demonstrates that the moduli obtained are independent of the boundary conditions of the tests. From Tables 17 and 18 it can be noted that average logarithmic slopes and

TABLE 7  
Torsion Modulus  
(psi  $\times 10^{-4}$ )

Specimen No.	Time (Seconds)						
	5	10	15	20	25	30	
1	2.06	1.38	1.12	1.02	0.90	0.84	
2	1.38	1.07	0.90	0.78	0.71	0.67	
3	2.14	1.52	1.31	1.07	0.98	0.90	
4	1.82	1.47	1.24	1.12	1.05	0.98	Stress = 23.1 psi
5	1.96	1.31	1.05	0.90	0.80	0.72	
6	2.14	1.63	1.32	1.18	1.05	0.98	
Avg.	1.92	1.40	1.16	1.01	0.92	0.85	
1	2.14	1.43	1.15	0.97	0.88	0.80	
2	1.54	1.12	0.94	0.85	0.78	0.73	
3	1.66	1.22	1.01	0.87	0.77	0.70	
4	1.66	1.26	1.04	0.92	0.83	0.77	Stress = 40.8 psi
5	1.89	1.38	1.12	0.98	0.88	0.83	
6	1.38	0.99	0.83	0.73	0.66	0.61	
Avg.	1.71	1.23	1.02	0.89	0.80	0.74	
1	1.98	1.29	1.06	0.90	0.78	0.71	
2	1.64	1.19	0.99	0.87	0.78	0.72	
3	1.99	1.10	0.93	0.80	0.72	0.64	
4	1.52	1.06	0.85	0.72	0.65	0.61	Stress = 58.3 psi
5	1.35	0.93	0.76	0.66	0.59	0.54	
6	1.35	0.96	0.80	0.69	0.63	0.58	
Avg.	1.64	1.09	0.90	0.77	0.69	0.63	



TABLE 8

Shear Modulus

(psi x 10<sup>-4</sup>)

Specimen No.	Time (Seconds)						
	5	10	15	20	25	30	
1	1.70	1.22	0.95	0.84	0.76	0.69	Stress = 23.1 psi
2	1.56	1.22	1.00	0.90	0.81	0.75	
3	1.56	1.16	0.95	0.84	0.75	0.69	
4	1.83	1.46	1.22	1.10	0.99	0.92	
5	1.46	1.16	0.95	0.88	0.81	0.73	
6	1.56	1.22	1.05	0.92	0.81	0.75	
Avg.	1.61	1.23	1.02	0.91	0.82	0.75	
1	1.42	1.04	0.86	0.74	0.66	0.60	Stress = 40.8 psi
2	1.56	1.20	1.00	0.89	0.80	0.74	
3	1.42	1.04	0.86	0.74	0.68	0.62	
4	1.73	1.56	1.07	0.94	0.84	0.80	
5	1.42	1.11	0.91	0.80	0.71	0.66	
6	1.56	1.11	0.94	0.82	0.74	0.68	
Avg.	1.52	1.18	0.94	0.82	0.74	0.68	
1	1.24	0.89	0.72	0.62	0.56	0.51	Stress = 58.3 psi
2	1.39	1.06	0.89	0.79	0.72	0.66	
3	1.48	1.06	0.85	0.74	0.66	0.59	
4	1.39	1.06	0.89	0.77	0.67	0.62	
5	1.27	0.93	0.78	0.68	0.62	0.56	
6	1.39	1.01	0.85	0.74	0.66	0.60	
Avg.	1.36	1.00	0.83	0.72	0.61	0.59	

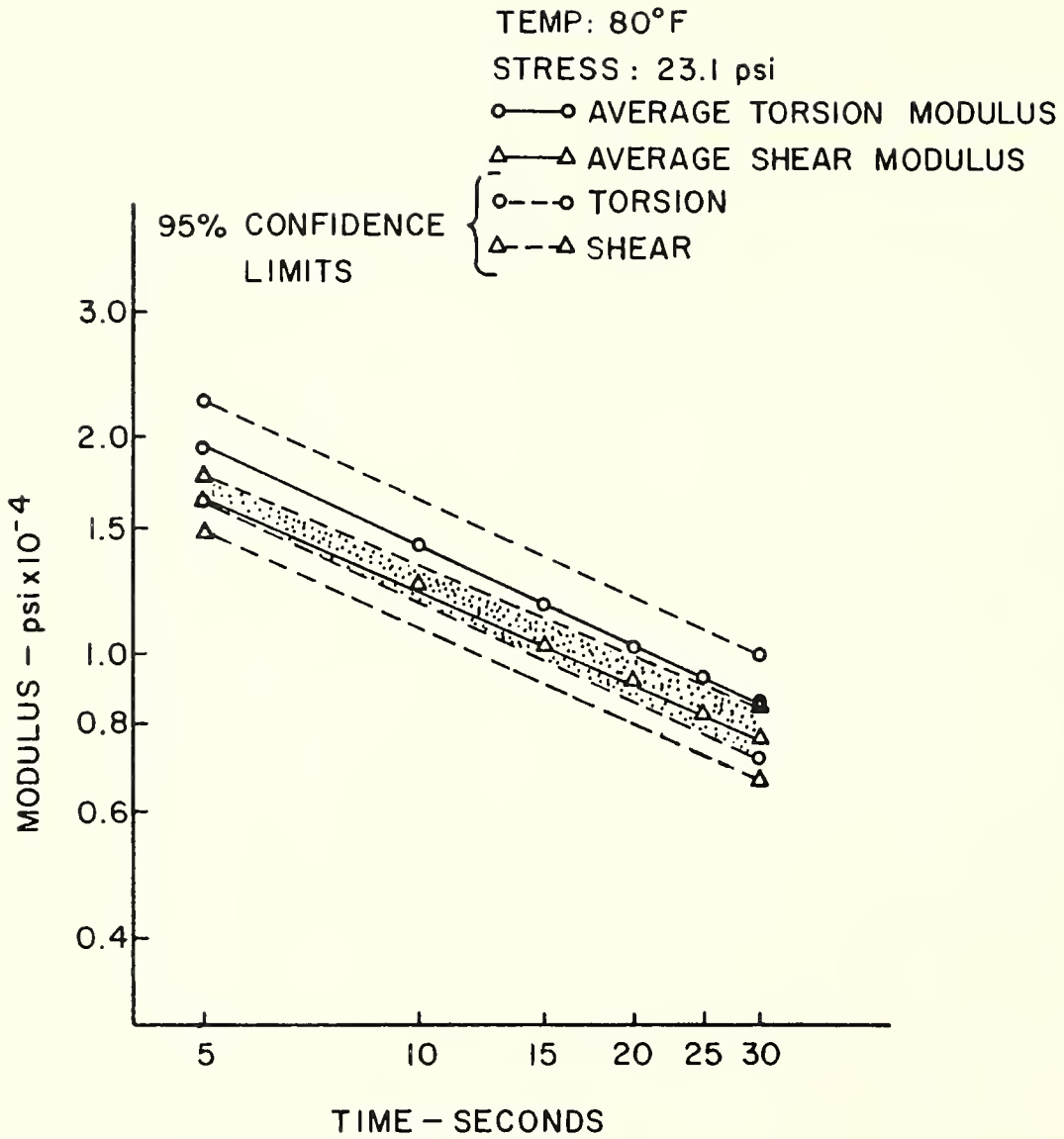


FIGURE 20. COMPARISON OF TORSION AND SHEAR MODULI - 23.1 psi

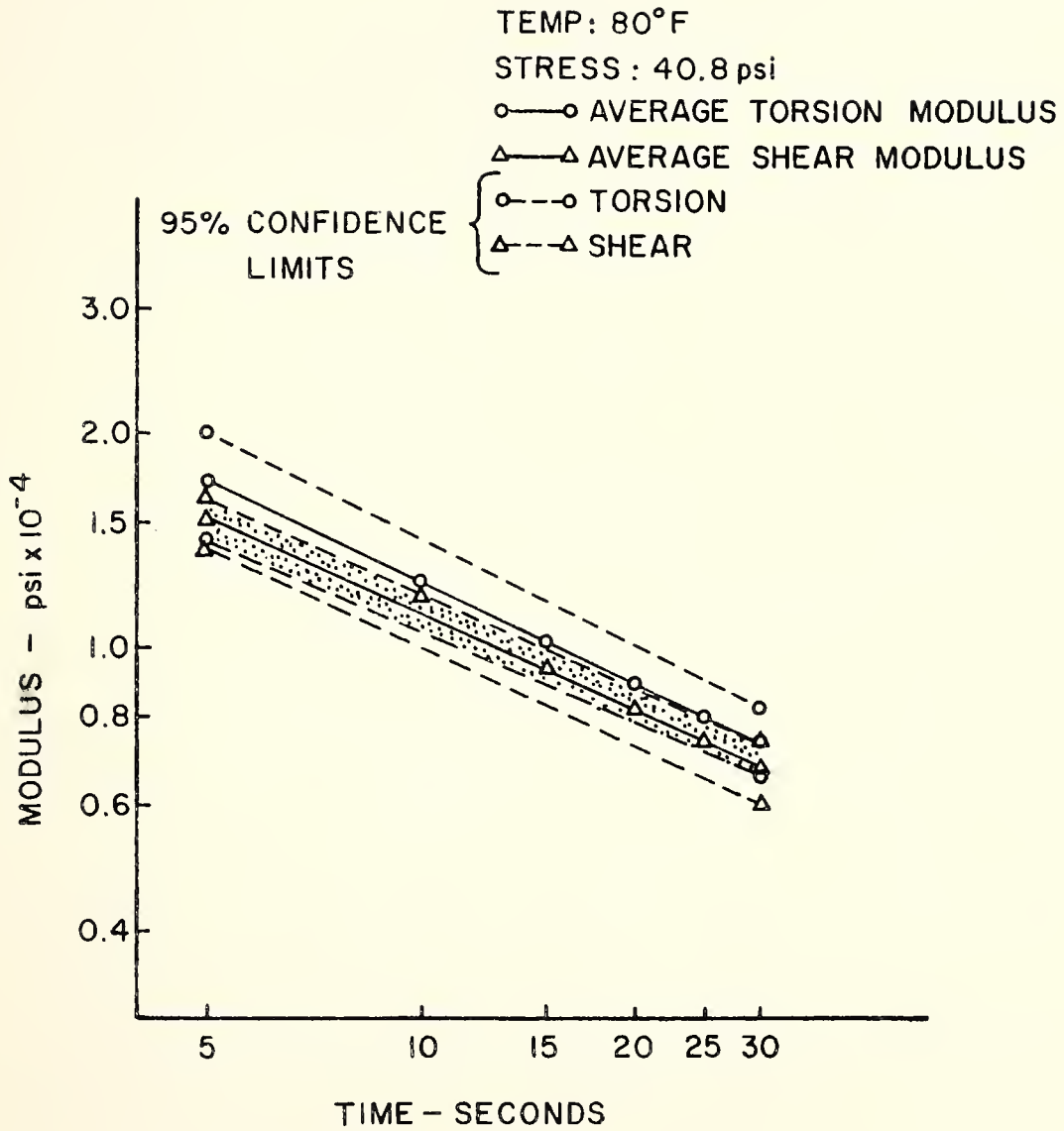


FIGURE 21. COMPARISON OF TORSION AND SHEAR MODULI - 40.8 psi

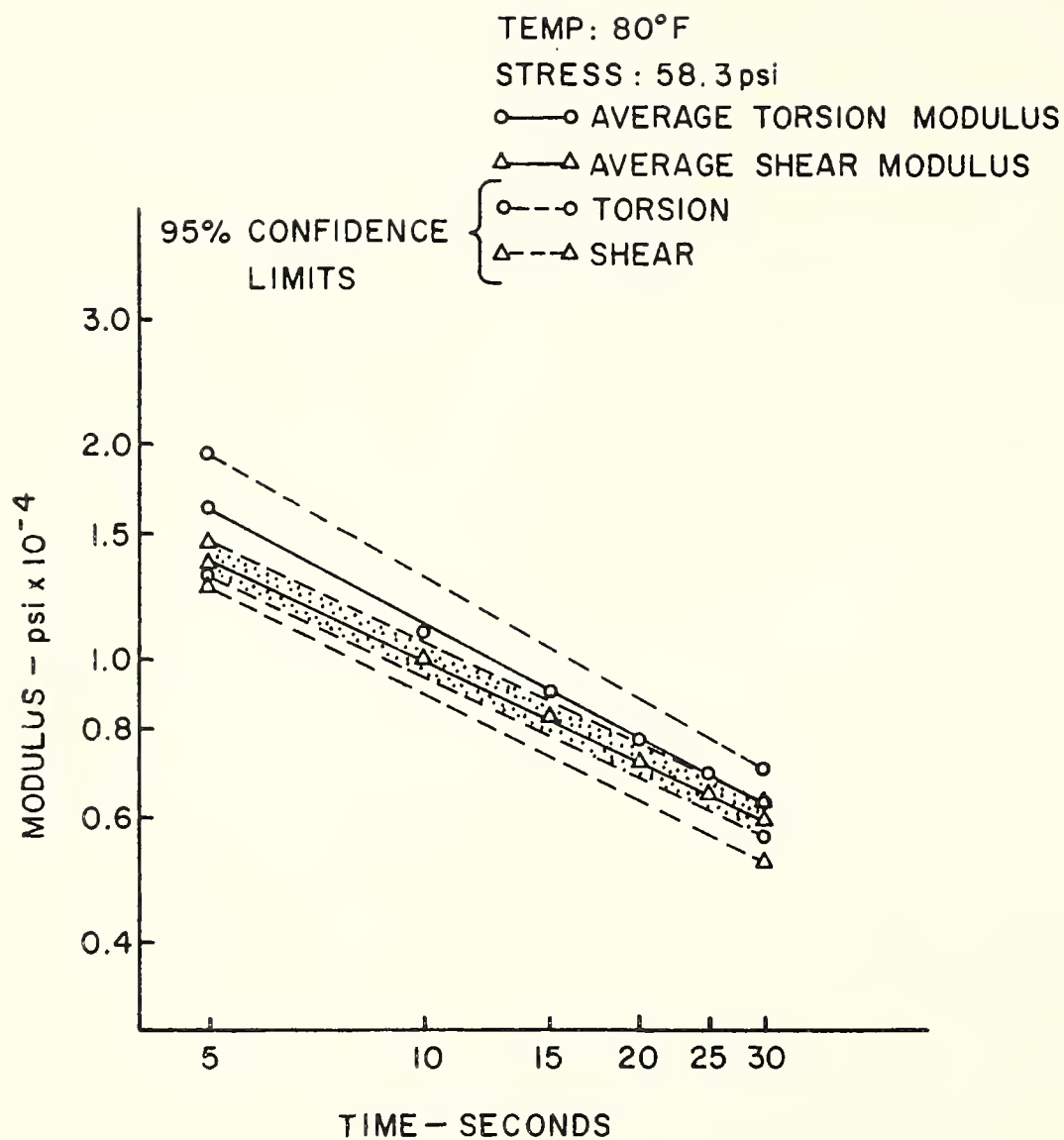


FIGURE 22. COMPARISON OF TORSION AND SHEAR MODULI - 58.3 psi

intercepts at 30 seconds decrease with increasing stress for both shear and torsion tests.

Figure 23 shows the three-dimensional character of the shear modulus when plotted as a function of time and stress for one temperature considered in testing. Data of this nature could be stored in the memory of an electronic computer and used to assist in predicting pavement and mixture performance.

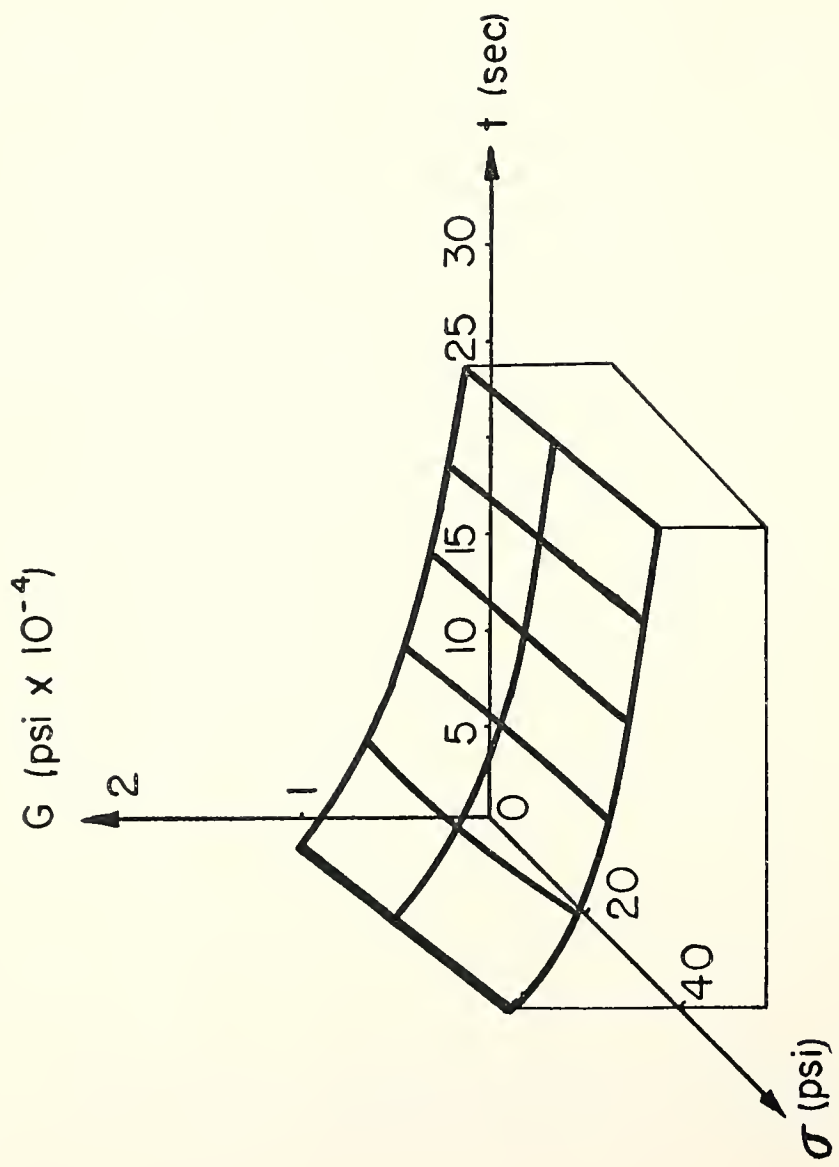


FIGURE 23. SHEAR MODULUS REPRESENTED AS A FUNCTION OF TIME AND STRESS AT 80°F.

## SUMMARY OF RESULTS AND CONCLUSIONS

The results and conclusions justified by data obtained in this study are summarized here. The scope of the study included one bituminous mixture, laboratory compacted, tested at three stress and three temperature levels, and for durations of loading up to thirty seconds. It should be recognized that these results and conclusions are known to be applicable only to the materials and testing procedures used in this investigation. Extrapolation of experimental results is not justified without further testing.

1. Six material coefficients exist and may be used for the description of the stress-deformation behavior of transversely anisotropic, statistically homogeneous, deformable materials subjected to small strains. The coefficients which relate stress to strain are as follows:

$$\begin{bmatrix} \epsilon_1 \\ \epsilon_2 \\ \epsilon_3 \\ \epsilon_4 \\ \epsilon_5 \\ \epsilon_6 \end{bmatrix} = \begin{bmatrix} \frac{1}{E_1} & \frac{\mu_{21}}{E_1} & \frac{\mu_{13}}{E_3} & 0 & 0 & 0 \\ \frac{\mu_{21}}{E_1} & \frac{1}{E_1} & \frac{\mu_{13}}{E_3} & 0 & 0 & 0 \\ \frac{\mu_{31}}{E_1} & \frac{\mu_{31}}{E_1} & \frac{1}{E_3} & 0 & 0 & 0 \\ 0 & 0 & 0 & \frac{1}{E_3} & 0 & 0 \\ 0 & 0 & 0 & 0 & \frac{1}{G_{13}} & 0 \\ 0 & 0 & 0 & 0 & 0 & \frac{2}{E_1} (1 - \mu_{21}) \end{bmatrix}$$

2. The methods of this investigation provide quantitative parameters that relate the common engineering concepts of stress and strain. The parameters can be used in the description, evaluation and design of bituminous mixtures for the prefailure conditions considered in the testing program.



Reliability of the parameters was established statistically for material coefficients obtained from shear and torsion tests.

3. It is feasible to determine the values of the six material coefficients by the testing methods utilized in this study. From determinations of the material coefficients, strains can be predicted, temperature and stress dependence of the bituminous mixture can be assessed and a measure of transverse anisotropy can be obtained. Tests include uniaxial compression tests, direct shear tests, torsion tests and uniaxial compression tests with volume change measurements.

4. For the bituminous mixture tested, stiffnesses in compression were greater in the direction of imposed compaction forces than in orthogonal directions indicating that assumptions of isotropy for bituminous mixtures are questionable. The logarithm of mixture stiffness was found to vary essentially linearly when plotted against the logarithm of time for the time interval from five to thirty seconds. Mixture stiffness also decreased with increasing stresses and test temperatures. Anisotropy appears to be independent of time, for the mixture tested, at the stress levels and temperatures used in the study.

5. A necessary condition for the invariance of the material coefficients was satisfied for the mixture used in this study. Both torsion and direct shear tests yielded essentially the same values for the shear modulus for three magnitudes of stress applied at the 80°F test temperature.

6. Poisson's ratios obtained from volumetric measurements and linear measurements did not agree and additional work is necessary to determine accurately the dependence of Poisson's ratios on temperature and applied stress for small strains. Data from volume change measurements indicate that Poisson's ratio is independent of time for the conditions of this test.

## ACKNOWLEDGMENTS

The authors wish to acknowledge the assistance of the Bureau of Public Roads, U. S. Department of Commerce, who supported the investigation with the Indiana State Highway Commission.

Laboratory testing and experimental techniques were carried out in the Bituminous Materials Laboratory of the Joint Highway Research Project at Purdue University, Lafayette, Indiana.

## REFERENCES CITED

1. Barden, Laing, "Stresses and Displacements in a Cross-anisotropic Soil," Geotechnique, Vol. 13, No. 3, December, 1963.
2. Bland, D. R., The Theory of Linear Viscoelasticity, Pergamon Press, New York, 1960.
3. Busching, H. W., "A Laboratory Investigation of the Structural Design of Bituminous Mixtures," Ph.D. Thesis, submitted to the Faculty of Purdue University, 1967.
4. Cady, Walter G., Piezoelectricity, Vol. 1, Dover Publications, New York, 1964.
5. Doyle, D. V., Drow, J. T. and McBurney, R. S., "Elastic Properties of Wood," Report No. 1528, Forest Products Laboratory, Madison, Wisconsin, 1956.
6. Elliott, H. A., "Three-dimensional Stress Distributions in Hexagonal Aeolotropic Crystals," Proceedings of the Cambridge Philosophical Society, Vol. 44, Part 4, 1948.
7. Greszskuk, L. B., "Effect of Material Orthotropy on the Directions of Principal Stresses and Strain," Paper presented at the Fifth Pacific Area National Meeting of the ASTM, Seattle, 1965.
8. Hearmon, R. F. S., An Introduction to Applied Anisotropic Elasticity, Oxford, London, 1961.
9. Jayne, B. A., Suddarth, S. K., "Mechanics of Fibrous Orthotropic Materials," Paper presented at Fifth Pacific Area National Meeting of the ASTM, Seattle, 1965.
10. Lal, N. B., "Two-Dimensional Stress-strain Relationships of a Fine Asphalt-Aggregate System," Ph.D. Thesis, submitted to the Faculty of Purdue University, 1965.
11. Leaderman, H., Elastic and Creep Properties of Filamentous Materials and Other High Polymers, The Textile Foundation, Washington, D. C., 1944.
12. Lee, A. R. and Marwick, A. H. D., "The Mechanical Properties of Bituminous Surfacing Materials Under Constant Stress," Journal of the Society of the Chemical Industry, London, 1937.

13. Lekhnitskii, S. G., Theory of Elasticity of An Anisotropic Elastic Body, Holden-Day, San Francisco, 1963.
14. Livneh, M. and Shklarsky, E., "The Bearing Capacity of Asphaltic Concrete Carpets," Proceedings, International Conference on the Structural Design of Asphalt Pavements, Ann Arbor, Michigan, 1962.
15. Love, A. E. H., A Treatise on the Mathematical Theory of Elasticity, Dover Publications, New York, 1944.
16. Meddelingen, LGM, "De Spanningverdeling in een Homogeen, Anisotroop Elastisch Halfmedium," Vol. 5, No. 2, 1960.
17. Mix Design Methods for Asphalt Concrete, The Asphalt Institute, College Park, Maryland, May, 1963.
18. Monismith, Carl, L., Alexander, R. L., and Secor, K. E., "Rheologic Behavior of Asphalt Concrete," Paper prepared for presentation at the Annual Meeting of the Association of Asphalt Paving Technologists, Minneapolis, 1966.
19. Papazian, H. S., "The Response of Linear Viscoelastic Materials in the Frequency Domain with Emphasis on Asphaltic Concrete," Proceedings of the International Conference on the Structural Design of Asphalt Pavements, Ann Arbor, Michigan, 1962.
20. Perloff, W. H. and Moavenzadeh, F., "Deflection of Viscoelastic Medium Due to a Moving Load," Paper prepared for the Second International Conference on the Structural Design of Asphalt Pavements, 1967.
21. Puzinauskas, V. P., "Influence of Mineral Aggregate Structure on Properties of Asphalt Paving Mixtures," Highway Research Board Record No. 51, Highway Research Board, 1964.
22. Roscoe, K. H. and Schofield, A. N., Discussion in Journal, Soil Mechanics and Foundation Section, American Society of Civil Engineers, January, 1964.
23. Schapery, R. A., "An Approximate Method of Stress Analysis for a Large Class of Problems in Viscoelasticity," Aeronautical and Engineering Science Report No. 62-18, Purdue University, 1963.
24. Sokolnikoff, I. S., Mathematical Theory of Elasticity, McGraw-Hill, New York, 1946.
25. "Stress-strain Relations in Wood and Plywood Considered as Orthotropic Materials," Report No. 1503, Forest Products Laboratory, Madison, Wisconsin, 1962.
26. Williams, M. L., "Structural Analysis of Viscoelastic Materials," Journal, AIAA Vol. 2, No. 5, 1964.

27. Wolf, K., "Distribution of Stress in a Half-plane and in a Half-space of Anisotropic Material," Zeitschrift für Angewandte Mathematik und Mechanik, Vol. 15, No. 5, 1935.
28. Wood, L. E. and Goetz, W. H., "Rheological Characteristics of a Sand-Asphalt Mixture," Proceedings, Association of Asphalt Paving Technologists, Vol. 28, 1959.

## APPENDIX

Notation

This appendix is included to specify the conventions used in defining stresses, strains, and various ratios and moduli that are discussed in the main body of the text.

A standard convention in matrix notation is to use the first subscript following a matrix element to designate the number of the row in which the element is located and the second subscript to designate the number of the column in which the element is located.

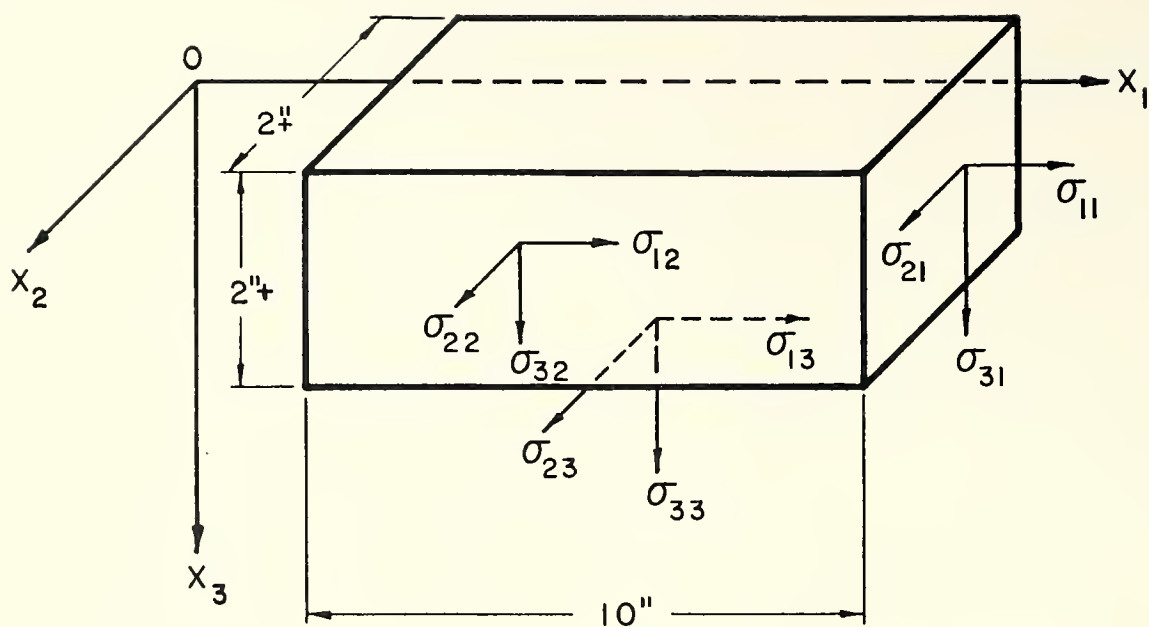
The orientation of the coordinate system in which stresses are described is shown in Figure 24. Referenced to this coordinate system is a sketch of the compacted beam of bituminous mixture from which test specimens were prepared.

The stresses shown on the beam illustrate the notation convention used throughout the discussion. In general,  $\sigma_{ij}$  are normal components of stress and  $\sigma_{ij}$  ( $i \neq j$ ) are tangential components.

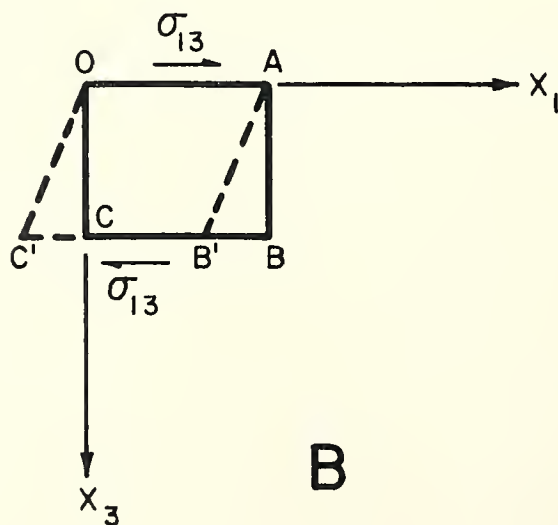
The strains,  $\epsilon_{ij}$ , are extensional strains defined as (change in length) per (original length). The components  $\epsilon_{ij}$  ( $i \neq j$ ) are shear strains and are defined diagrammatically in the lower portion of Figure 24.

When the shear stress  $\sigma_{13}$  acts as shown in the figure, a distortion occurs in the element causing the unit square ABCO to change into the rhombus AB'C'O. The angles BAB' and COC' are each equal to  $\epsilon_{13}$ .

The subscript convention for Poisson's ratio involves two numbers. In general,  $\mu_{ij}$  denotes Poisson's ratio,  $\epsilon_i/\epsilon_j$ , when the stress is directed along the coordinate axis  $x_j$ . The time- and temperature-dependent shear modulus is denoted by the letter  $G_{13}$ , while the moduli defined from normal strains in the  $x_1$  and  $x_3$  directions are designated  $E_1$  and  $E_3$ , respectively.



A



B

FIGURE 24. ORIENTATION OF BEAM OF  
COMPACTED BITUMINOUS MATERIAL  
SHOWING NOTATION CONVENTION





